

ARBRL-MR-2800

BRL

AD

TECHNICAL
LIBRARY

MEMORANDUM REPORT ARBRL-MR-2800

140-GHZ ATTENUATION AND OPTICAL VISIBILITY
MEASUREMENTS OF FOG, RAIN AND SNOW

Victor W. Richard
John E. Kammerer
Richard G. Reitz

December 1977

Approved for public release; distribution unlimited.

USA ARMAMENT RESEARCH AND DEVELOPMENT COMMAND
USA BALLISTIC RESEARCH LABORATORY
ABERDEEN PROVING GROUND, MARYLAND

Destroy this report when it is no longer needed.
Do not return it to the originator.

Secondary distribution of this report by originating
or sponsoring activity is prohibited.

Additional copies of this report may be obtained
from the National Technical Information Service,
U.S. Department of Commerce, Springfield, Virginia
22161.

The findings in this report are not to be construed as
an official Department of the Army position, unless
so designated by other authorized documents.

*The use of trade names or manufacturers' names in this report
does not constitute indorsement of any commercial product.*

UNCLASSIFIED

SECURITY CLASSIFICATION OF THIS PAGE (When Data Entered)

REPORT DOCUMENTATION PAGE		READ INSTRUCTIONS BEFORE COMPLETING FORM
1. REPORT NUMBER MEMORANDUM REPORT ARBRL-MR-2800	2. GOVT ACCESSION NO.	3. RECIPIENT'S CATALOG NUMBER
4. TITLE (and Subtitle) 140-GHz Attenuation and Optical Visibility Measurements of Fog, Rain and Snow		5. TYPE OF REPORT & PERIOD COVERED
		6. PERFORMING ORG. REPORT NUMBER
7. AUTHOR(s) Victor W. Richard, John E. Kammerer, Richard G. Reitz		8. CONTRACT OR GRANT NUMBER(s)
9. PERFORMING ORGANIZATION NAME AND ADDRESS US Army Ballistic Research Laboratory Aberdeen Proving Ground, MD 21005		10. PROGRAM ELEMENT, PROJECT, TASK AREA & WORK UNIT NUMBERS 1M362303A214, Task 00 001AJ 1M161102AH43, Task 06 001AJ
11. CONTROLLING OFFICE NAME AND ADDRESS US Army Materiel Development & Readiness Command 5001 Eisenhower Avenue Alexandria, VA 22333		12. REPORT DATE DECEMBER 1977
		13. NUMBER OF PAGES 84
14. MONITORING AGENCY NAME & ADDRESS (if different from Controlling Office)		15. SECURITY CLASS. (of this report) UNCLASSIFIED
		15a. DECLASSIFICATION/DOWNGRADING SCHEDULE
16. DISTRIBUTION STATEMENT (of this Report) Approved for public release; distribution unlimited.		
17. DISTRIBUTION STATEMENT (of the abstract entered in Block 20, if different from Report)		
18. SUPPLEMENTARY NOTES		
19. KEY WORDS (Continue on reverse side if necessary and identify by block number) Rain attenuation at 140 GHz Atmospheric attenuation at 140 GHz Fog attenuation at 140 GHz Rain, fog and snow attenuation calculation at Snow attenuation at 140 GHz 140 GHz Rain, fog and snow visibility		
20. ABSTRACT (Continue on reverse side if necessary and identify by block number) (idk/kst) The attenuation of fog, rain and snow has been measured at 140 GHz (2.1 mm wavelength) for rainfall intensities varying from drizzles up to 20 mm/hr and over a wide range of fog and snowfall intensities. Measured attenuation data are compared with theoretically derived attenuation data. Optical visibility and 140 GHz attenuation measurements were made simultaneously, providing comparisons between optical and millimetre wave system capabilities under degraded weather conditions. (Continued)		

UNCLASSIFIED

SECURITY CLASSIFICATION OF THIS PAGE(When Data Entered)

A brief review of the theoretical and experimental work of a number of authors on the computation and measurement of fog, rain and snow attenuation at 140 GHz is presented. An extensive reference and bibliography list is given which includes a number of articles from Soviet open literature.

UNCLASSIFIED

SECURITY CLASSIFICATION OF THIS PAGE(When Data Entered)

TABLE OF CONTENTS

	<u>Page</u>
LIST OF ILLUSTRATIONS	5
LIST OF TABLES.	7
I. INTRODUCTION	9
II. EXPERIMENT DESCRIPTION	9
A. General	9
B. 140-GHz Attenuation Measurements.	11
C. Visibility Measurement.	16
D. Rain and Snow Intensity Measurement	21
E. Data Recording	21
III. RESULTS DISCUSSION	23
A. Fog Attenuation and Visibility.	23
1. Fog Measurements.	23
2. Fog Characteristics	26
3. Fog Attenuation Calculations.	29
B. Rain Attenuation and Visibility	38
1. Rain Attenuation Measurements	38
2. Rain Attenuation Calculation.	44
3. Temperature Effect on Rain Attenuation	47
4. Wind Effect on Rain Attenuation	48
5. Rain Visibility Measurements.	48
C. Snow Attenuation and Visibility	51
1. Snow Measurements	51
2. Snow Attenuation Calculation.	57
IV. CONCLUSIONS	60
V. ACKNOWLEDGEMENTS.	65
REFERENCES.	66
BIBLIOGRAPHY.	71
DISTRIBUTION LIST	79

LIST OF ILLUSTRATIONS

<u>Figure</u>		<u>Page</u>
1	Field Site for 140 GHz Attenuation and Visibility Measurements	10
2	140 GHz Propagation Attenuation Measuring System	12
3	140 GHz Transmitter and Antenna	13
4	140 GHz Receiving Station and Light Source	14
5	140 GHz Receiver	15
6	Telephotometer for Transmittance Measurements	19
7	Atmospheric Attenuation Versus Meteorological Range	20
8	Tipping Bucket Rain Guage with Heater	22
9	Measured 140 GHz Fog Attenuation	24
10	Measured and Calculated 35 and 140 GHz Fog Attenuation	25
11	Fog Visibility Versus Liquid Water Content	30
12	Calculated Fog Attenuation Versus Frequency	35
13	Calculated Fog Attenuation Versus Visibility	36
14	Ratio of Fog Attenuation at T° to Attenuation at 0° C Versus Frequency	37
15	Fog Attenuation Coefficient Versus Temperature	39
16	Measured One-Way Attenuation 140 GHz Versus Rainfall Rate	40
17	Measured Attenuation of Lucite Window Versus Rainfall Rate	42
18	Measured Attenuation of Wetted Lucite Window	42
19	Measured and Calculated Rain Attenuation by Tolbert, Sanders and BRL	43
20	Calculated Rain Attenuation Versus Rainfall Rate	45

LIST OF ILLUSTRATIONS

<u>Figure</u>		<u>Page</u>
21	Measured Rain Attenuation Versus Visibility	49
22	Visibility Versus Rainfall Rate	50
23	Chart Record of 140 GHz Attenuation, Visibility and Tipping Bucket Pulses During Snow Storm	52
24	140 GHz Attenuation, Visibility and Equivalent Rainfall Rate Versus Time	53
25	140 GHz Snow Attenuation and Visibility Versus Melted Snow Equivalent Rainfall Rate	54
26	Wet Snow 140 GHz Attenuation Versus Visibility	56
27	Measured Snow Attenuation Versus Frequency	58
28	Rain, Fog, and Atmospheric Attenuation Versus Frequency .	62
29	140 GHz Water Vapor Attenuation Versus Relative Humidity and Temperature	63

LIST OF TABLES

<u>Table</u>		<u>Page</u>
I	Haze, Cloud, Fog and Rain Drop-Size Characteristics . . .	27
II	Fog Attenuation Coefficient, dB/km/g/m ³ at 20° C	34

I. INTRODUCTION

This report presents the results of a field experiment conducted by the Ballistic Research Laboratory (BRL) to measure the attenuation of fog, rain and snow at 140 GHz (2.1 millimetres wavelength) and the associated optical visibility. The objective of this experiment was to determine the quantitative relationship between 140 GHz propagation attenuation and fog, rain and snow intensity and visibility. These data were needed to obtain a more accurate and complete quantitative understanding of the environmental effects and performance limiting boundaries on radar, guidance and homing systems operating at 140 GHz.

A number of military applications of millimetre wave systems are based on their unique ability to operate successfully when the visibility is poor. Thus, in addition to the use of the conventional criteria for defining the intensity of fog, rain, or snow storms by their water content or rate of rainfall, optical visibility was also used. In many weapon systems applications, visibility is more easily determined in the field and a more practical criterion of weather conditions than water content or rainfall rate.

In order to accurately evaluate the maximum operating range and quality of performance of 140 GHz systems, additional experimental data were needed on the effects of degraded weather to supplement the meager amount of experimental data available and to serve as a check on the theoretically derived data currently available. A review of the literature on propagation attenuation at 140 GHz disclosed a number of theoretical studies and some rain measurements but no substantiating measurements were found for fog and snow.

II. EXPERIMENT DESCRIPTION

A. General

Measurements of attenuation and visibility during degraded weather were made during the period of January through April 1975. Usable data were obtained from nine rainstorms of long duration, four days with fog, and one heavy snow storm of over three hours duration.

The measurements were made over a flat, open field as shown in Figure 1. Figure 1 also shows the 140 GHz receiving site and the light source co-located at a range of 725 metres from the 140 GHz transmitter. A second light source was located at a range of 68 metres for use when the fog was extremely dense.

The attenuation caused by fog, rain, or snow was determined by continuously recording the received 140 GHz signal level before, during and after each storm and measuring the difference in the signal level between clear weather and stormy weather conditions. Thus, only the additional



Figure 1. Field Site for 140 GHz Attenuation and Visibility Measurements

attenuation caused by degraded weather was measured. The initial propagation attenuation caused by normal, fair weather atmospheric absorption was not obtained.

Visibility was measured by continuously recording the light level received from a light source in the field at either 725- or 68-metre range.

B. 140 GHz Attenuation Measurement

A block diagram of the 140 GHz propagation measuring system is shown in Figure 2. A klystron transmitter with an average power output of 50 milliwatts was used. The klystron was modulated with a 1000-Hz square wave derived from a tuning fork source with a 0.1% frequency stability. Frequency stabilization of the modulation was necessary because of the very narrow bandwidth 1000-Hz amplifiers used in the receiver.

A portion of the klystron output was sampled with a 10-dB directional coupler, detected, and monitored as a check on the amplitude stability of the klystron output. A precision variable attenuator was inserted between the klystron and the antenna for amplitude calibration of the receiver output records.

The transmitting antenna was a 41-cm diameter, Fresnel zone plate lens illuminated with a small horn, as shown in Figure 3. This antenna had a beamwidth of 0.38 degrees and a gain of 53 dB. The transmitting antenna height above ground was 1.5 metres.

The 140 GHz receiver was located at a range of 725 metres from the transmitter in an instrumentation trailer as shown in Figure 4. The receiving antenna, shown in Figure 5, was a lens antenna identical to the transmitting antenna. The received signal was demodulated by a tuned diode detector. The 1000-Hz detected signal was amplified in a low-noise, narrow-bandwidth amplifier of the type used for VSWR indicators. Considerable experimentation was required to select a low loss detector and low noise 1000-Hz amplifier to provide a signal-to-noise ratio adequate to conduct the experiment. The crystal-video receiver, although not as sensitive as a superheterodyne, had the advantage of simplicity, stability and no need for an operator at the site.

The output of the tuned 1000-Hz amplifier was fed by coaxial cable back to the transmitter site where it was again amplified in a tuned 1000-Hz amplifier, rectified, filtered and recorded on paper charts.

A reference calibration signal from the 1000-Hz tuning fork oscillator could be switched into the tuned amplifiers for gain stability checks.

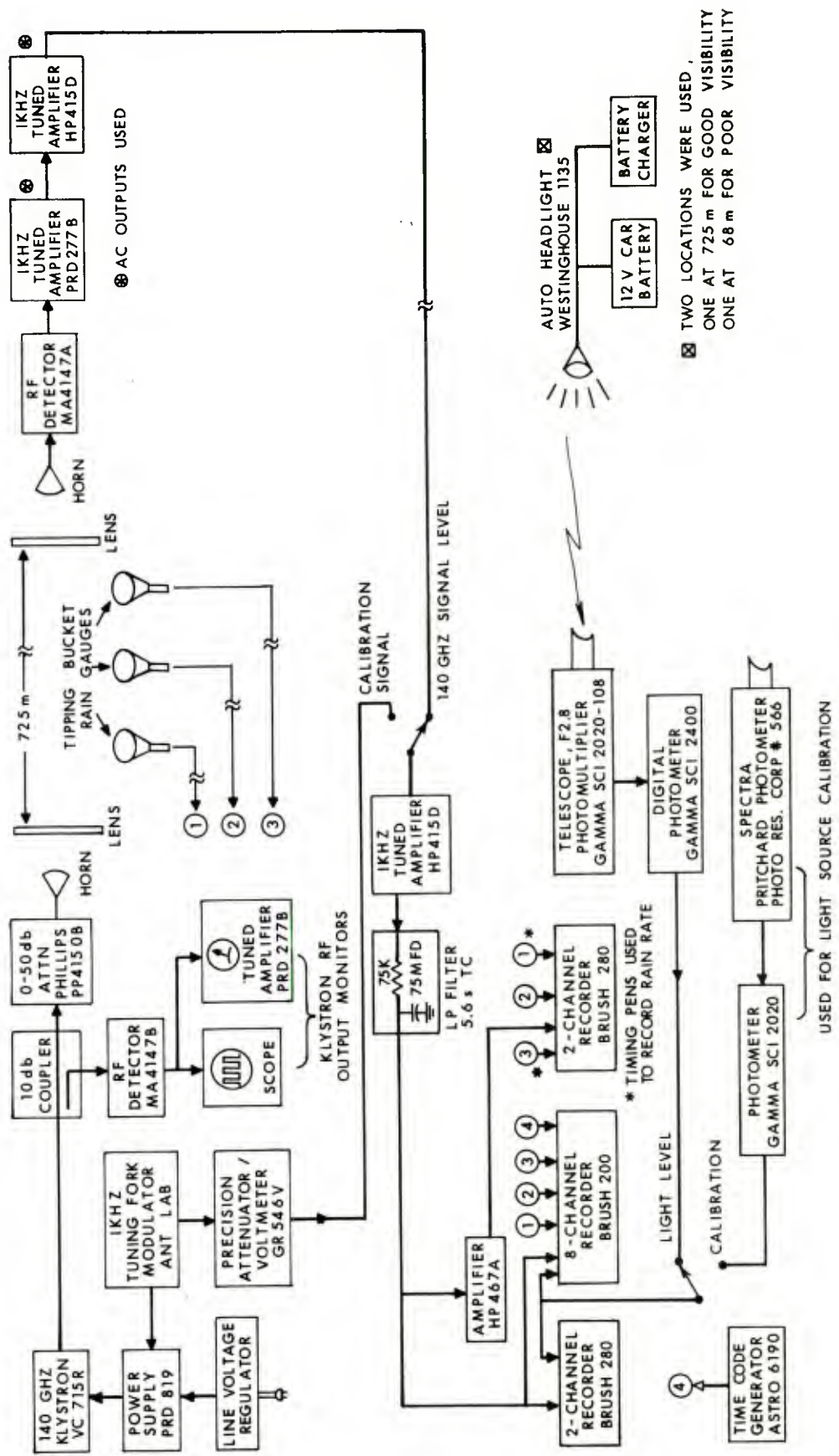


Figure 2. 140 GHz Propagation Attenuation Measuring System

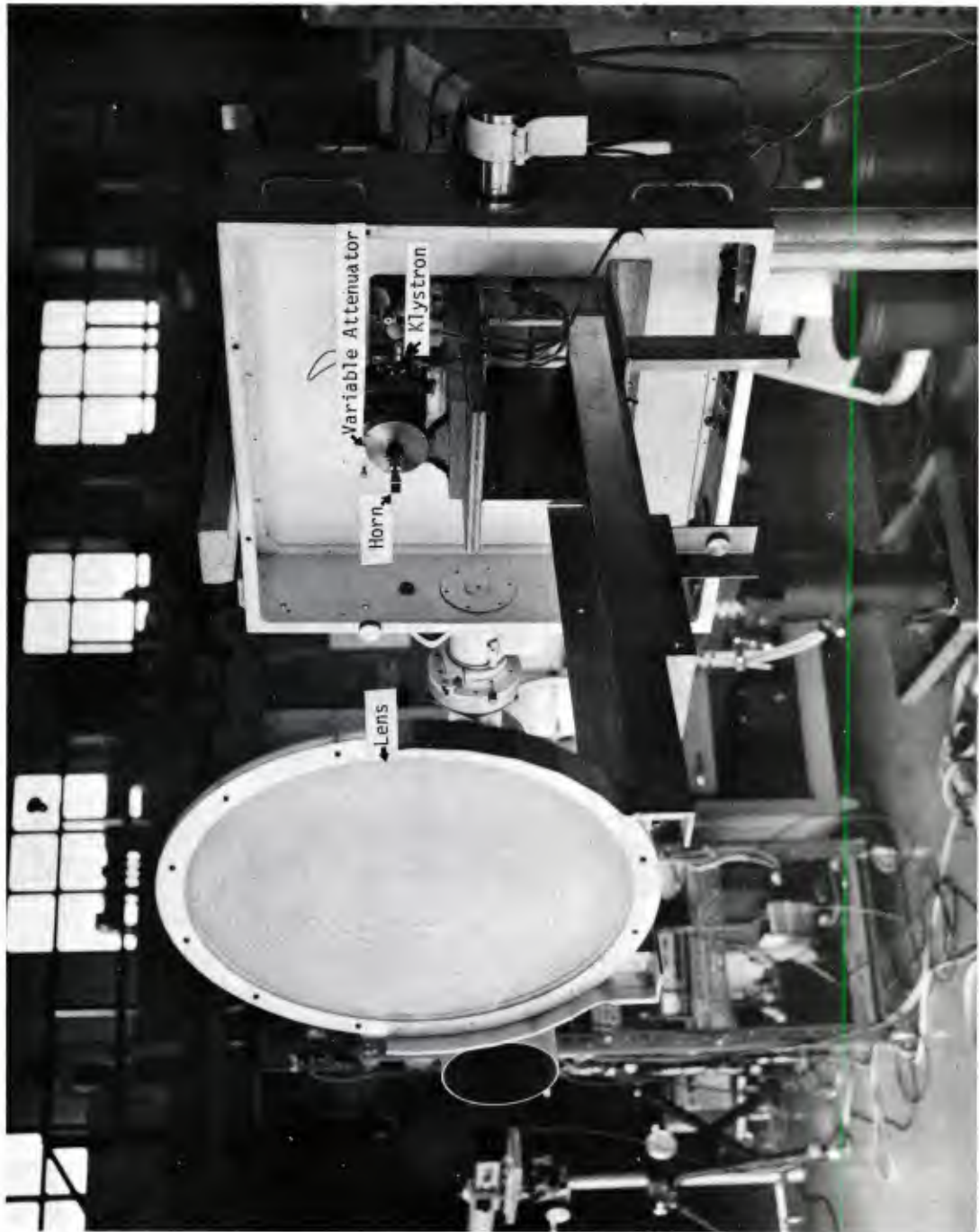


Figure 3. 140 GHz Transmitter and Antenna



Figure 4. 140 GHz Receiving Station and Light Source

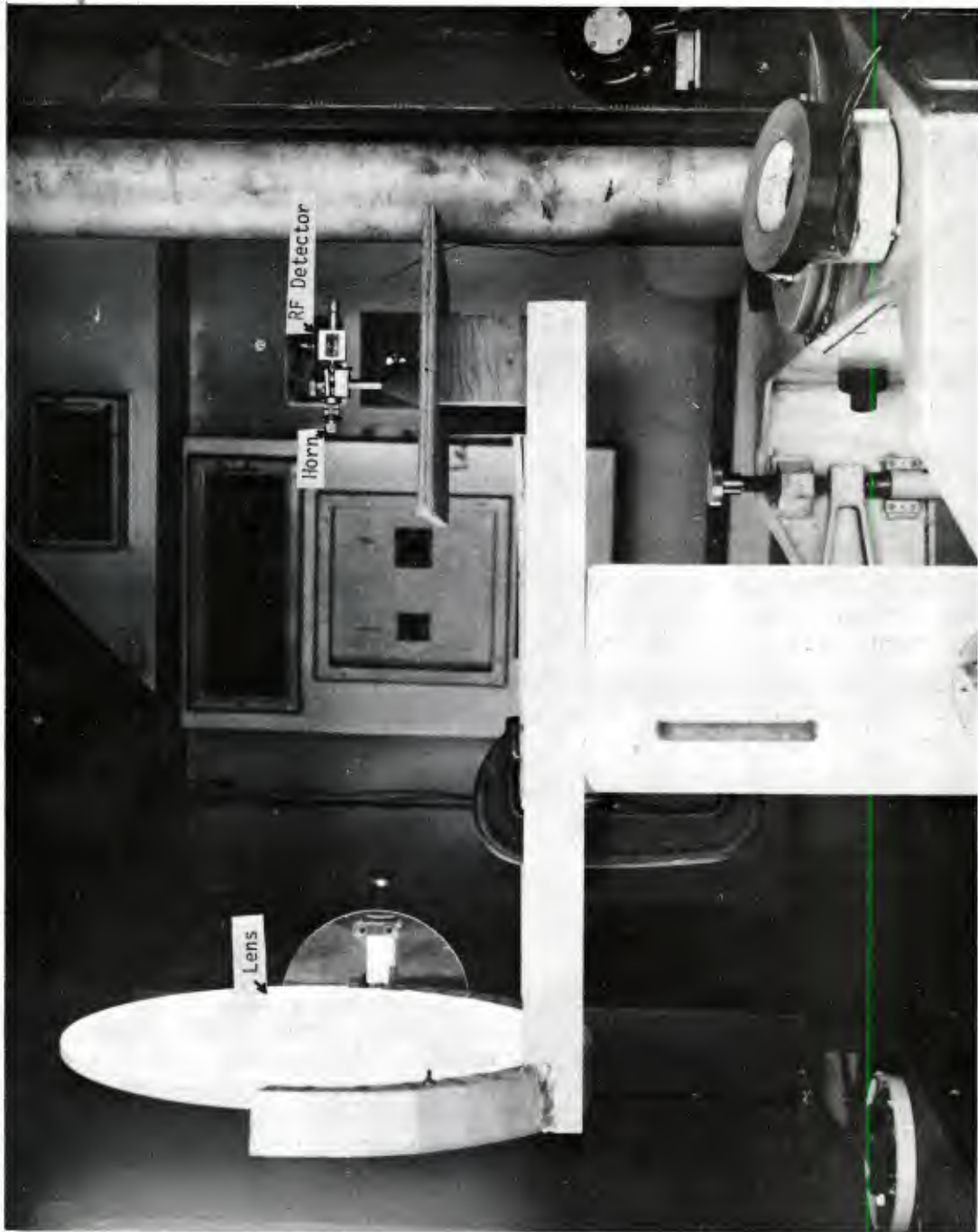


Figure 5. 140 GHz Receiver

C. Visibility Measurements

The definition of visual range is that distance at which the contrast between a target and its background is equal to the threshold contrast of a human observer under daytime conditions, or, in equation form

$$VR = \frac{1}{\sigma} \ln \frac{|C|}{\epsilon} \quad (1)$$

where VR \equiv visual range

σ \equiv atmospheric attenuation coefficient

C \equiv contrast between the target and its background

ϵ \equiv contrast threshold of the eye.

The meteorological range is an empirically consistent measure of the visual range where C is equal to -1 (the contrast of a flat black object as viewed against the horizon sky) and ϵ is equal to 0.02. Contrast is defined by the equation

$$C = \frac{\beta - \beta'}{\beta'} \quad (2)$$

where β is the luminance of an object and β' is the luminance of the background. For an ideal black object, the luminance of the object is zero and the contrast is -1. The value of $\epsilon = 0.02$ for daytime conditions is based upon Blackwell's¹ extensive studies involving contrast and human observers. The meteorological range in equation form, substituting constants for C and ϵ , becomes

$$MR = \frac{3.912}{\sigma} \quad (3)$$

where MR is the meteorological range and σ is the atmospheric attenuation coefficient.

The method for determining the meteorological range for this experiment was a transmissometer which employed a light source and a light-sensing instrument to measure the luminance of the source. For a constant output of the light source and a constant separation between the source and photometer, the amount of light which the photometer measures corresponds to the transmittance of the atmosphere between the source and receiver.

¹Middleton, Visibility Through the Atmosphere, Univ. of Toronto Press, 1958.

The transmittance is related to the atmospheric attenuation coefficient by the relation

$$\sigma = \frac{1}{r_0} \ln \left(\frac{1}{T} \right) \quad (4)$$

where σ is the atmospheric attenuation coefficient, r_0 is the distance between the source and the photometer, and T is the transmittance over the path length r_0 .

Combining equations (3) and (4), the transmittance is related to the meteorological range by

$$MR = \frac{3.912 r_0}{\ln(1/T)} \quad (5)$$

Solving (5) for T , the result is

$$T = e^{-3.912 \frac{r_0}{MR}} \quad (6)$$

Differentiating and dividing by T

$$\frac{dT}{T} = \frac{3.912 r_0}{MR} \frac{d(MR)}{MR} \quad \text{or}$$

$$\frac{MR}{r_0} = 3.912 \frac{d(MR)}{MR} \frac{1}{\frac{(dT)}{T}} \quad (7)$$

Assuming that T can be measured to an accuracy of ± 1 percent and the value of MR is desired to ± 10 percent, upon substitution of these values into (7), the ratio MR/r_0 should not be greater than 40. If the short base line (68 metres) is used for dense fogs, inaccuracies are encountered when the meteorological range is determined for light rain conditions with meteorological ranges of possibly 10 kilometres. If a base line is used that is too long, the light will be completely attenuated by dense fogs. To avoid this problem, two base lines and two light sources were employed - one base line was 68 metres and the other was 725 metres. The two base lines permitted adequate coverage from **dense fog** through light haze conditions.

Each light source was a Westinghouse No. 4435, 12 volt automotive spotlight. A 100 ampere-hour, 12-volt battery under continuous charge provided a very stable voltage supply for each light source.

The light sensing system consisted of a Gamma 2400 Telephotometer with a telescope, photomultiplier tube, and a photopic correction filter as shown in Figure 6. The photopic filter matched the spectral response of the photometer to that of the human eye.

The luminance of each light source was measured on a very clear night, in order to determine the luminance with as little atmospheric attenuation as possible. A standard lamp was used to calibrate the photometer before measurements were made. When an aerosol such as fog was in the area, the luminance of the source was measured and the value of the transmittance calculated by

$$T = \frac{\beta_1}{\beta_0} \quad (8)$$

where T is the transmittance, β is the luminance of the light in the presence of an aerosol, and β_0 is the luminance of the light in a clear atmosphere.

The value of the meteorological range was then calculated by substituting that value of transmittance into equation (5). If the aerosol became so dense that the light source at the 725 metre range could not be seen, the photometer was used to measure the luminance of the light source at the 68 metre range.

In addition to the light sources, several olive drab painted vehicles were located at varying distances near the line of sight of the photometer to determine how well the empirical meteorological range compared with the human eye. The values of the meteorological range by the two methods were comparable.

The value of attenuation can be used in place of transmittance according to the relation

$$A = 1 - T \quad (9)$$

where A is the attenuation, and T is the transmittance. Figure 7 shows the attenuation versus meteorological range, where the meteorological range is a multiple of the base line r_0 . The luminance was measured continuously and the value of meteorological range was determined for each instant of time which was of interest.

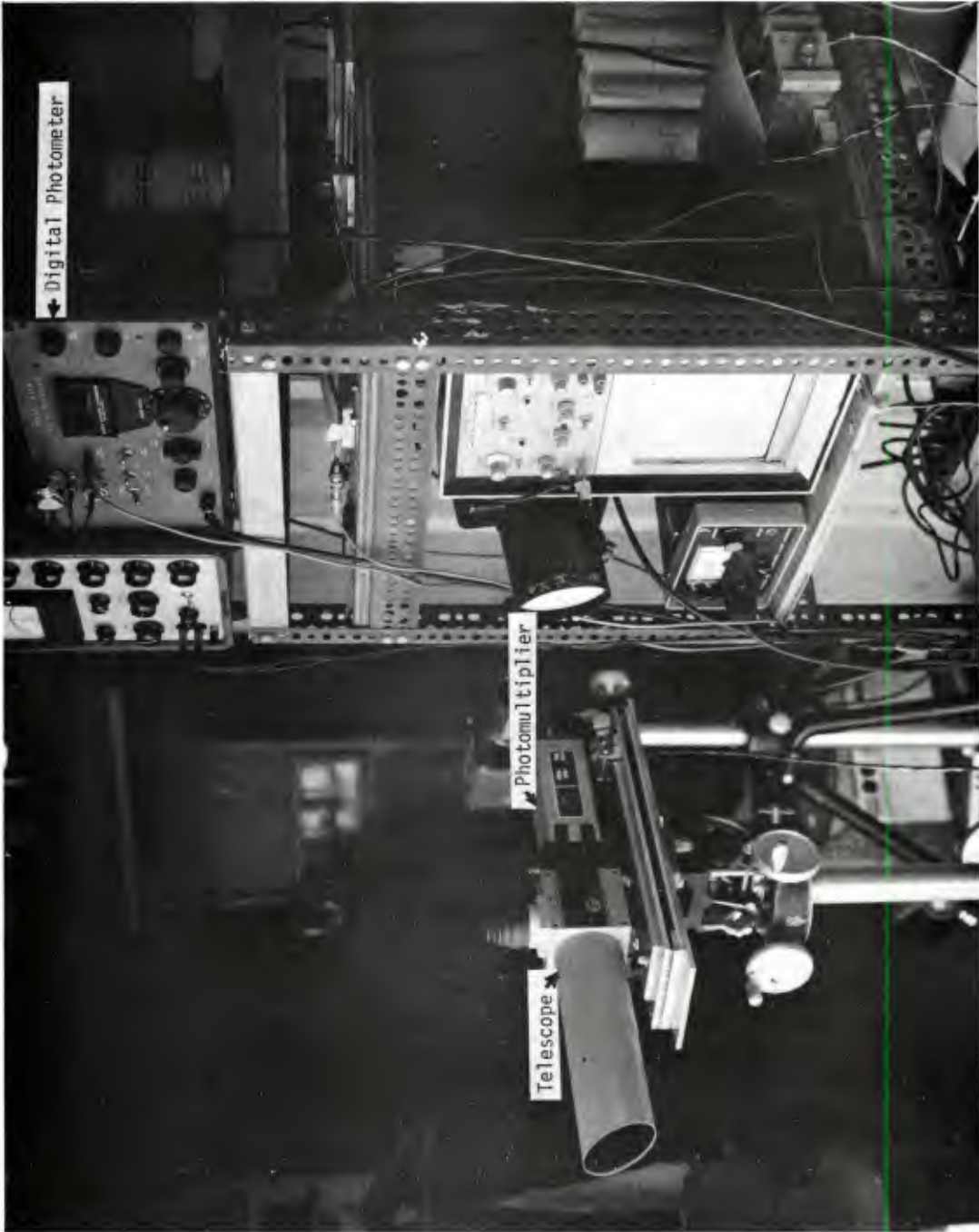


Figure 6. Telephotometer for Transmittance Measurements

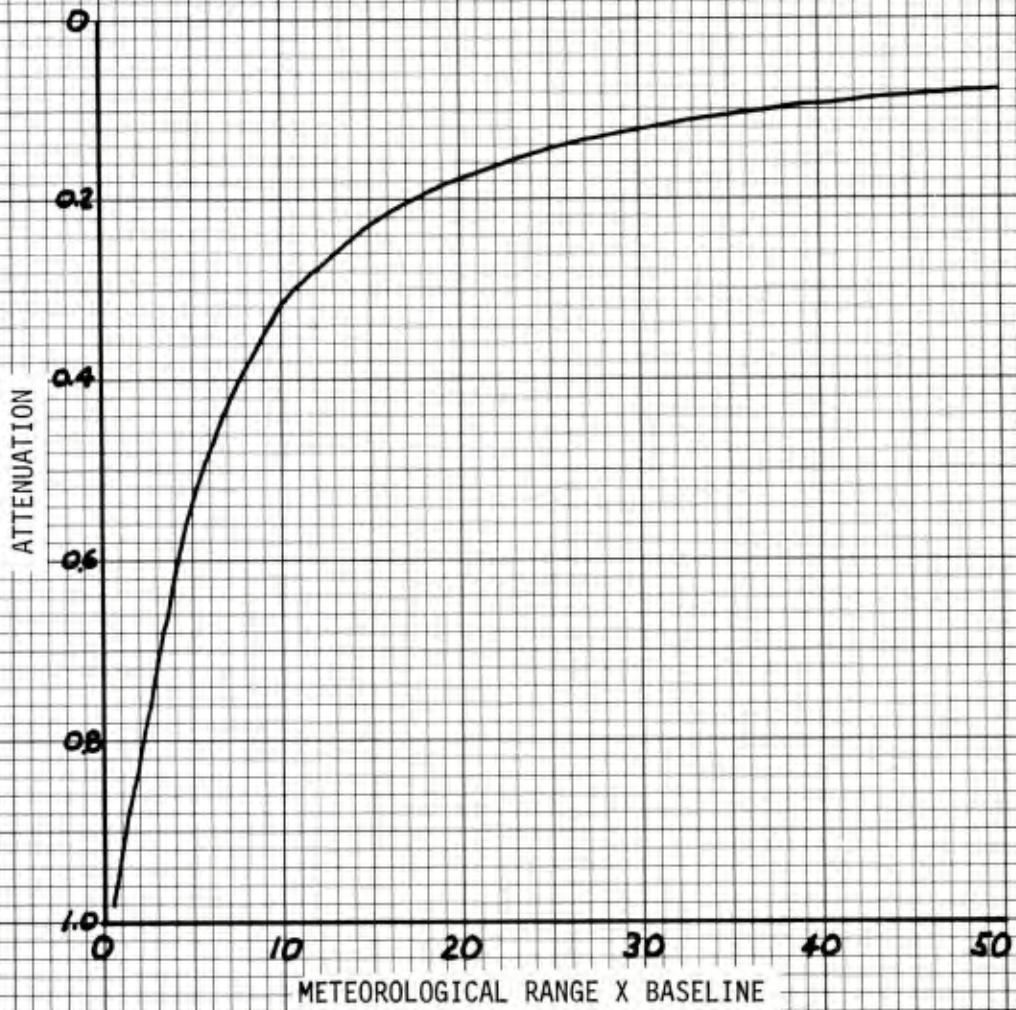


Figure 7. Atmospheric Attenuation Versus Meteorological Range

D. Rain and Snow Intensity Measurement

Rainfall rate was measured with three tipping bucket rain gauges, one gauge was located at each end of the propagation path and one midway along the path. The tipping buckets were modified to increase their sensitivity by a factor of ten by increasing the orifice area by a factor of ten with a 63.1-cm diameter funnel, as shown in Figure 8. Previous experience with these rain gauges, which have a sensitivity of one tip per 0.254 mm of rain collected, indicated the need for a much faster tipping rate for accurately measuring light rainfall rates and for correlating rainfall rate with RF propagation phenomena. The ten-to-one increase in orifice area increased the sensitivity to 0.0254 mm of rain per tip. The time between tips for a rainfall rate of 1 mm/hr was 1.5 minutes, compared with 15 minutes for the unmodified rain gauges.

The modification does result in the inability of the buckets to tip fast enough to accurately measure rainfall rates above about 10 mm/hr, plus the requirement for a rather fast chart recorder paper speed to keep the bucket-tip pulses separated sufficiently to read.

Snowfall intensity was determined by measuring the equivalent rainfall rate of the snow and visibility range. Heating cords were wrapped around the body of the tipping bucket rain gauge and the funnel to melt the snow, as shown in Figure 8. Thus, the water content of the snow was measured in terms of equivalent rainfall rate. This is a commonly used criteria of snowfall intensity but does not give any information regarding the snowflake sizes, density, or fall rate which are also needed to completely characterize snow.

E. Data Recording

An eight-channel paper chart recorder was used to record the pulses from the tipping bucket gauges and the analog outputs from the 140 GHz receiver and the photometer. Supplemental recordings of the 140-GHz signal and the photometer output were made on two additional two-channel paper chart recorders to give improved data reading resolution. Prior to and immediately after recording data, a calibration was made by stepping the RF attenuator through a range of 0 to 10 dB in one-half dB increments. The photometer had an accurate linear output in terms of foot-lamberts, so only a full scale identification was required for the visibility chart recordings. A test 1000-Hz signal was periodically switched into the received signal amplifier system to check the gain stability and make the necessary gain adjustments to compensate for amplifier and recorder drift. In practice, very few gain adjustments were required; the overall amplifier and recorder system drift over several hours was approximately one-tenth of a dB, which was about the reading definition of the chart recordings.



Figure 8. Tipping Bucket Rain Gauge With Heater

III. RESULTS DISCUSSION

A. Fog Attenuation and Visibility

1. Fog Measurements. Visibility and 140-GHz attenuation measurements were made on four days when the fog was present over the same 725-metre land path used for rain attenuation measurements. The data taken during the four foggy days are shown in Figure 9. The equation of the best fit line is

$$\alpha_f = 0.13 V^{-1.43} \quad (10)$$

where α_f is the fog attenuation in dB/km and V is the visibility in kilometres.

There is considerable scatter of the data points, which is not unusual when characterizing fog by its visibility. Visibility is strongly dependent on the small-droplet concentration which may vary greatly in different fogs, whereas 140-GHz attenuation is more strongly dependent on the total liquid water content. Thus, similar attenuation may result from a wide range of visibility conditions. This is illustrated in Figure 9 where an attenuation of 0.2 dB/km occurred for visibility ranging from 0.32 to 2 km. Under more dense fog conditions, the spread in the visibility was not so great; e.g., at 0.8- to 0.9-dB/km attenuation, the visibility ranged only from 0.15 to 0.3 km. Non-homogeneous fog along the propagation path could also have contributed to the scatter of the data observed. There does not seem to be a significant difference between the data from the four days, except at the longer visibility range, where the visibility on 24 March was greater than for the other days for the same attenuation.

No other measured 140-GHz fog attenuation data were found for comparison from the literature search conducted, the closest in frequency being measurements of fog attenuation at 35 GHz by Robinson.² Figure 10 shows Robinson's 35 GHz data and the 140 GHz data from Figure 9. There is considerable similarity between the data at these two frequencies when compared with their respective calculated attenuation curves. The measured fog attenuation for each frequency is higher than calculated, assuming radiation type fog which applies to fog which forms over land. The slope of the 140 GHz measured data is close to the calculated line between 0.09 and 0.3 kilometres visibility range. It appears that the fog attenuation measured during these two experiments falls somewhere

²Robinson, N.P., "Measurements of the Effect of Rain, Snow, and Fogs on 8.6 mm Radar Echoes," *Proc. IEE*, London, 203B, Paper No. 189R, 709-714, September 1955.

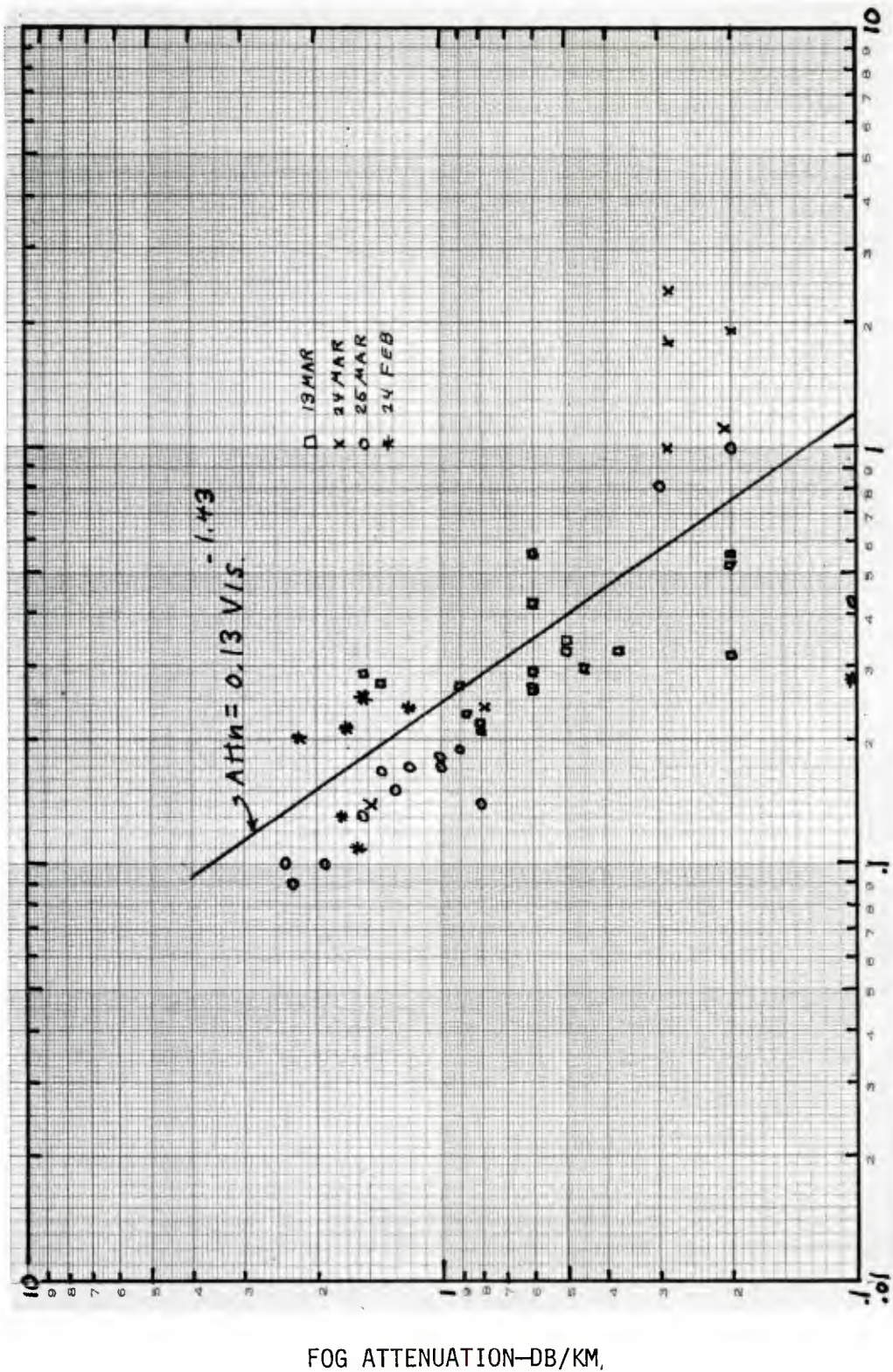


Figure 9. Measured 140 GHz Fog Attenuation

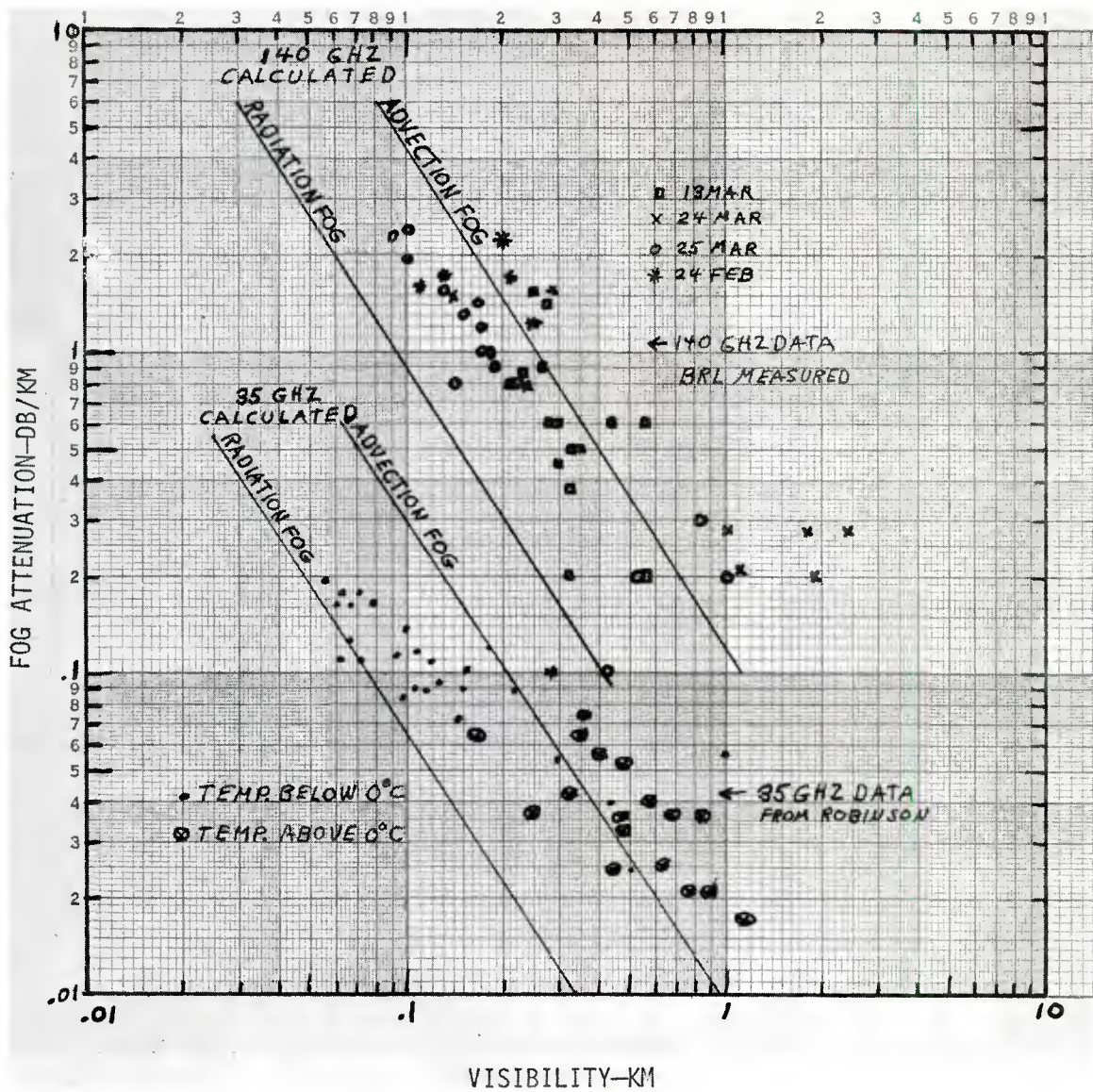


Figure 10. Measured and Calculated 35 and 140 GHz Fog Attenuation

between radiation and advection fog characteristics, with a trend toward the advection fog curve for the longer range visibility conditions. Advection type fog normally forms over water and has larger water droplets than radiation. The derivation of the calculated curves in Figure 10 is given in the following section.

2. Fog Characteristics. Attenuation of electromagnetic waves by fog, haze, and clouds is caused by the absorption and scattering of energy from condensed water droplets suspended in the atmosphere. Fog can be characterized by its drop-size distribution, droplet density, and liquid water content.

The wavelength dependence of attenuation by condensed water is a function of the size, density and temperature of the water droplets. At millimetre wavelengths, where the drop sizes are small compared with the wavelength, the attenuation depends primarily on the density and temperature of the water droplets and is not very sensitive to drop-size. However, at optical wavelengths, the attenuation is very sensitive to drop-size, particularly the small droplets.

Wide ranges of water droplet sizes and concentrations are encountered in the atmosphere, depending upon the meteorological and geographical conditions. The analysis and understanding of millimetre wave and optical attenuation is aided by a comparison of the size and the volume concentration of water droplets for haze, clouds, fog and rain as shown in Table I from Lukes³ and Koester and Kosowsky.^{4,5}

Haze has very small droplets, in the range of 0.01 to 3 microns diameter, which do not cause significant attenuation at millimetre wavelengths but cause some reduction in visibility.

Clouds and fog are composed of droplets in the range of 1 to 65 microns, but the density is much greater in fog, 200×10^4 droplets/m³ compared with 100×10^6 droplets/m³ in clouds.

³Lukes, G.D., "Penetrability of Haze, Fog, Clouds, and Precipitation on Radiant Energy over the Spectral Range 0.1 Micron to 10 Centimeters," The Center for Naval Analyses, Univ. of Rochester, Study No. 61, May 1968, AD 847 658

⁴Koester, K.L. and Kosowsky, L.H., "Attenuation of Millimeter Waves in Fog," 14th Radar Meteorology Conf., Tucson, AZ, 17-20 Nov 1970; also, Norden Div of United Aircraft Corp., Rpt X32052, 10 August 1970.

⁵Koester, K.L. and Kosowsky, L.H., "Millimeter Wave Propagation in Fog," IEEE, Ant. & Prop. Symp., 20-24 Sep 1971, Los Angeles, CA; Norden Div. United Aircraft Rpt X32059, 14 June 1971.

TABLE I. HAZE, CLOUD, FOG AND RAIN CHARACTERISTICS

Parameter	Haze	Clouds	Radiation Fog	Advection Fog	Drizzle 0.25mm/hr	Light Rain 1mm/hr	Medium Rain 4mm/hr	Heavy Rain 16mm/hr
Drop Diameter Range, Microns	0.01-3	1-30	5-35	7-65	5-2000	10-2500	10-3000	10-3500
Typical Drop Concentration, per m ³	100 x 10 ⁶	100 x 10 ⁶	200 x 10 ⁹	40 x 10 ⁹	275	360	500	650
Typical Maximum Water Content, g/m ²	--	0.5	1	0.4	0.025	0.1	0.3	1.0
Water Content for 200 Meters Visibility	--	--	0.04	0.18	0.025	0.07	0.25	0.8
Visibility at 0.1 g/m ³ , m	--	380	110	280	8500	6300	7600	1100

Fog which forms over land is called radiation fog which, typically, has droplet sizes between 5 and 35 microns diameter, with an average diameter of 10 microns and a density of 200×10^9 droplets/m³.

Fog which forms over water is called advection fog, which, typically, has droplet sizes ranging from 7 to 65 microns with an average diameter of 20 microns and a density of 40×10^9 droplets/m³. Because of the greater number of larger droplets, advection fog has a greater visibility than radiation fog with the same water content. For a given visibility, advection fog has a larger water content than radiation fog and consequently a higher attenuation at millimetre wavelengths. According to Koester and Kosowsky,^{4,5} the fog attenuation and visibility data derived by Ryde and Ryde⁶ and quoted in commonly used references such as Kerr⁷ and Skolnik⁸ apply to advection fogs which have a minimum visibility of about 100 metres. Very dense fogs, with visibilities of less than 100 metres are generally radiation fogs which have a different visibility-water content relationship.

The use of optical visibility as a criterion for fog conditions is not completely definitive for purposes of correlation with millimetre wave attenuation. Fogs of a specified attenuation, i.e. water content, can vary greatly in visibility because they can be composed of different droplet sizes. However, because one very important criterion for evaluating millimetre wave systems is their capability of operating under limited conditions, the use of visibility to characterize the fog was used in the experiment described in this report to determine the limits of attenuation uncertainty with respect to attenuation. Another factor in this choice of visibility as the fog criterion was the relative ease of making continuous measurements of visibility compared with making a continuous recording of drop-size distribution or liquid water content that was representative over the propagation path.

An estimate of the liquid water content of fog can be made from visibility data if the type of fog is known. An empirically derived equation for the relationship between radiation fog and visibility by Eldridge⁹ is

⁶Ryde, J.W. and Ryde, D., "Attenuation of Centimeter and Millimeter Waves by Rain, Fog, and Clouds," Tech Rpt 8670, British General Electric Co., Wembley, England, May 1945; also, earlier report, GEC No. 7831, Oct 1941, Ryde & Ryde. See also C.R. Burrows and S.S. Atwood, Radio Wave Propagation, Academic Press, NY, Vol II, Chap 5, 1949.

⁷Kerr, D.E., Propagation of Short Radio Waves, McGraw Hill, NY, 1951.

⁸Skolnik, M., Introduction to Radar Systems, McGraw Hill, NY, 1962.

⁹Eldridge, R.G., "Haze and Fog Aerosol Distributions," J. Atmospheric Sci., 23, 605-613, 1966.

$$V = 0.024 M^{-0.65} \quad (11)$$

where V is the visibility in kilometres and M is the liquid water content in grams per cubic metre. Ryde and Ryde's⁵ equation for advection fog is

$$V = 0.054 M^{-0.699} \quad (12)$$

These equations are shown graphically in Figure 11. The line for advection fog stops at 0.4 g/m^3 because, according to Mason,¹⁰ the liquid water content of advection fog does not exceed this value. Consequently, the visibility of advection fog will not be less than 100 metres. Koester and Kosowsky^{4,5} state that the use of the advection fog relationship between visibility and water content for very dense fogs, where the visibility is less than 100 metres and the radiation fog relationship actually applies, will result in excessively large values of water content and attenuation. They report measurements at 70 GHz that substantiate the use of the radiation fog assumption for very dense fogs.

3. Fog Attenuation Calculations. The attenuation of condensed water droplets in the atmosphere can be calculated using Rayleigh scattering theory when droplet diameter and wavelength criteria are met. Since haze, clouds and fog droplet sizes are no greater than 100 microns, which is small compared with the wavelength of 2.1 mm, the Rayleigh approximation can be used and the equation for fog attenuation derived by Atlas¹¹ applies where

$$\alpha_F = \frac{81.86 \text{ Im}(-K)}{\lambda \rho} M \text{ dB/km} \quad (13)$$

where $\alpha_F \equiv$ fog attenuation, dB/km

$\text{Im}(-K) \equiv$ imaginary part of absorption coefficient, K

$\lambda \equiv$ wavelength

$\rho \equiv$ density of water

¹⁰Mason, B.J., *The Physics of Clouds*, Oxford, Clarendon Press, 1957.

¹¹Atlas, D., "Advances in Radar Meteorology," *Advances in Geophysics*, Vol. 10, 317-478, Academic Press, NY, 1964.

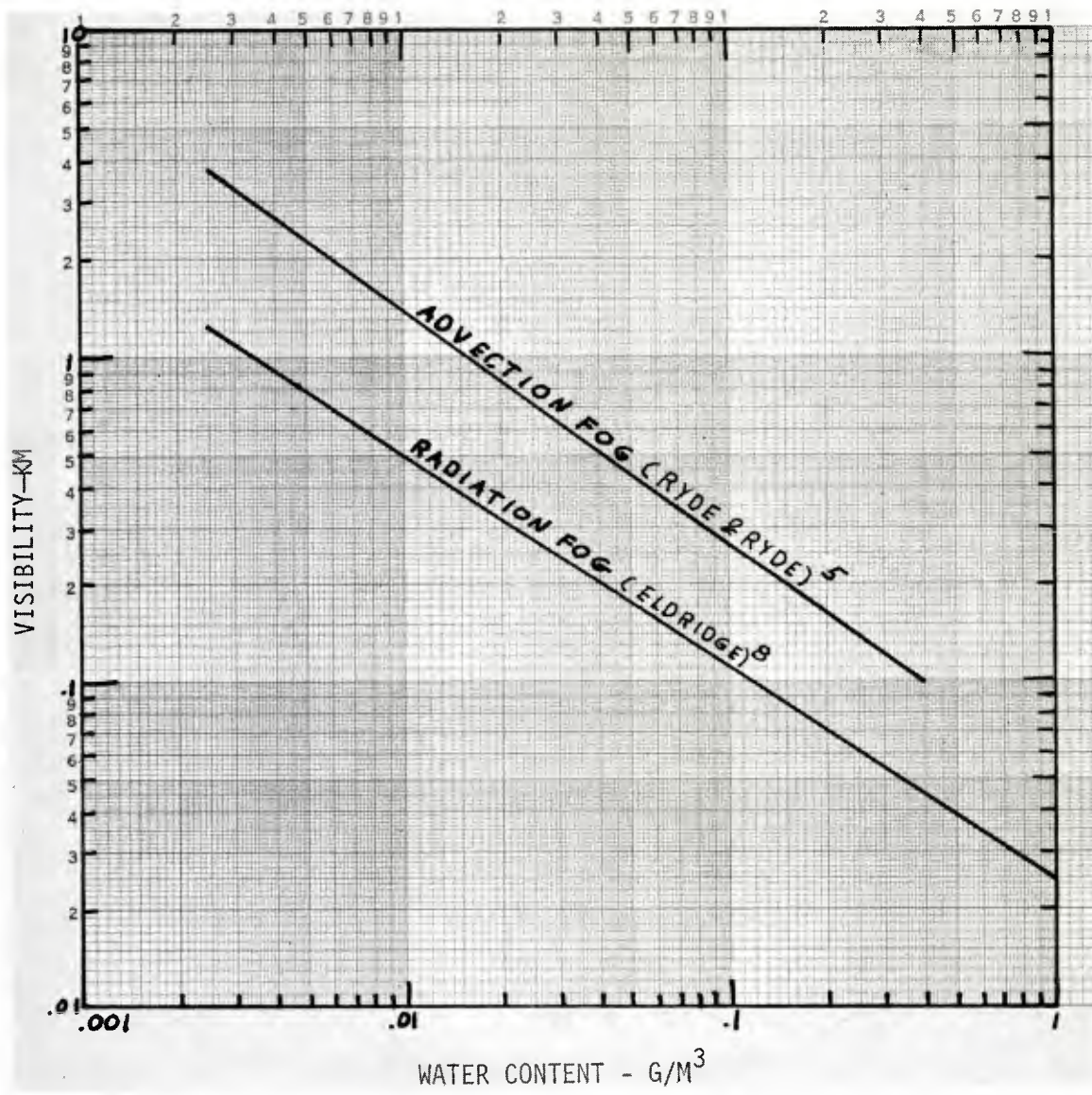


Figure 11. Fog Visibility Versus Liquid Water Content

The absorption coefficient, K , can be expressed in terms of the complex index of refraction of water, m , as

$$K = (m^2 - 1)/(m^2 + 2) \quad (14)$$

The complex refractive index of water can be expressed in terms of the complex dielectric constant of water, ϵ_c , using the Debye formula,

$$m^2 = \epsilon_c = \frac{\epsilon_0 - \epsilon_\infty}{1 + J \frac{\Delta\lambda}{\lambda}} + \epsilon_\infty \quad (15)$$

where $\Delta\lambda \equiv$ transition wavelength (line width)

$$\Delta\lambda = 2\pi c T_r \frac{\epsilon_0 + 2}{\epsilon_\infty + 2} \quad (16)$$

$T_r \equiv$ relaxation time of water molecules

$\epsilon_0 \equiv$ static dielectric constant at $\omega \ll \frac{1}{T_r}$

$\epsilon_\infty \equiv$ optical dielectric constant at $\omega \gg \frac{1}{T_r}$

$\omega \equiv$ angular frequency corresponding to λ

$c \equiv$ velocity of light

$\lambda \equiv$ wavelength

The accuracy of the evaluation of the complex index of refraction of water directly determines the accuracy of the calculation of fog attenuation. Values for ϵ_0 , ϵ_∞ and $\Delta\lambda$ needed for the evaluation of the complex dielectric constant are available from a number of sources, each slightly different, depending on the experimental data and computation procedures used.

Saxton and Lane,¹² Saxton,¹³ and Lane and Saxton¹⁴ are commonly used sources of refractive index of water up to millimetre wavelengths. Lukes³ gives a detailed review of many sources of refractive index of water data over the spectral range of 10 cm to 0.1 micron wavelength. Chamberlain, et al¹⁵ report on experimental data that does not follow the commonly used Debye formula. Deirmendjian^{16,17} and Mitchell¹⁸ have calculated complex index of refraction of water values for 3 to 300 GHz at temperatures between 0° and 40° C.

Several Russian authors have reported on their experimentally derived index of refraction of water data. Stanevich and Yaroslavskii¹⁹ report on measured data over the range of 40 to 2500 microns as well as

¹²Saxton, J.A. and Lane, J.A., "The Anomalous Dispersion of Water at Very High Radio-Frequencies," Meteorological Factors in Radio Wave Propagation, Physical Society, London, Parts I, II, and III, 1946.

¹³Saxton, L.A., "Dielectric Dispersion in Pure Polar Liquids at Very High Radio-Frequencies, II. Relation of Experimental Results to Theory," Proc. Royal Soc., A, 213, p 473, 1952.

¹⁴Lane, J.A. and Saxton, J.A., "Dielectric Dispersion in Pure Polar Liquids at Very High Radio-Frequencies. I. Measurements on Water, Methyl and Ethyl Alcohols," Proc. Royal Soc., 213, p 400, 1952; also, J. Opt. Soc Am., 56, No. 10, p 1398, 1966.

¹⁵Chamberlain, J.E., et al, "Submillimetre Absorption and Dispersion of Liquid Water," Nature, 210, 790-791, May 21, 1966.

¹⁶Deirmendjian, D., "Complete Microwave Scattering and Extinction Properties of Polydispersed Cloud and Rain Elements," The Rand Corp., R-422-PR, Dec 1963.

¹⁷Deirmendjian, D., Electromagnetic Scattering and Spherical Polydispersions, American Elsevier Pub. Co. Inc., NY, 1969.

¹⁸Mitchell, R.A., "Radar Meteorology of Millimetre Wavelengths," Aerospace Corp., Rpt TR-669(6236-46)-9, Air Force Rpt SSD-TR-66-117, June 1966. AD 488 085. NOTE: Figure 4 rain attenuation at 1mm wavelength is in error according to Mitchell's later report, "Remote Sensing of Rain by Radar," TR-0158(3525-09)-1, AF No. SAMSO-TR-68-115, January 1968.

¹⁹Stanevich, A.E., and Yaroslavskii, N.G., "Absorption of Liquid Water in the Lone-Wavelength Part of the Infrared Spectrum (42-2000 microns)," Optics and Spectroscopy, 10, 278-279, April 1961.

a review of many other sources of data. Malyshenko and Wackser²⁰ report on their computations of the complex dielectric constant of water at millimetre and submillimetre wavelengths using a modified Debye formula that includes water molecule resonance effects. Their own experimental data are also used.

A number of authors have reported on computations of fog attenuation at millimetre wavelengths based on equation (13), with each using slightly different values for the complex index of refraction of water from different sources of experimental data. Table II lists calculated fog attenuation between 15 and 3000 GHz by Koester and Kosowsky,^{4,5} Kerr,⁷ Hogg,²¹ Dudzinsky,²² Wilcox²³ and Rogers.²⁴ The attenuation is given as an attenuation coefficient in units of dB/km/g/m³ rather than for a particular liquid water content. Fog attenuation is linearly proportional to the liquid water content, as can be seen in equation (13).

A curve of fog attenuation versus frequency is shown in Figure 12, based on a best fit to the data in Table II. Figure 13 shows calculated fog attenuation for 35, 70, 95, 150 and 300 GHz versus visibility based on data from Figures 10 and 11.

There is a temperature effect on fog attenuation that is largest at the lower frequencies and interestingly goes through zero at about 150 GHz. Fog attenuation versus temperature data from Kerr,⁷ Mitchell,¹⁸ and Koester and Kosowsky^{4,5} are shown in Figure 14 in the form of the ratio of attenuation at temperatures between 10° and 40° C to the attenuation at 0° C as a function of frequency. This ratio is largest at

²⁰Malyshenko, Y.I. and Wachser, I.K., "Calculation of the Dielectric Constant of Water in the Submillimetre Range of Radio Waves," Ukrain. Phys., 15, No. 5, 1970.

²¹Chu, T.S., and Hogg, D.C., "Effects of Precipitation at 0.63, 3.5 and 10.6 Microns," BSTJ, 47, No. 5, May-June 1968, 723-759.

²²Dudzinsky, S.J., *Atmospheric Effects on Terrestrial Millimetre-Wave Communications*, Rand Corp. Rpt. R-1335-ARPA, Mar 1974.

²³Wilcox, F., "Millimetre Wave Radar," Proj. No. 1709-74-Db, JERA-2048, Goodyear Aerospace Corp., Arizona Division, Litchfield Park, AZ., 85340, 10 April 1975.

²⁴Rogers, T.F., "An Estimate of the Influence of the Atmosphere on Airborne Reconnaissance Radar Performance," Prop. Lab., Air Force Cambridge Res. Ctr., 4 Jan 1953.

TABLE II. FOG ATTENUATION COEFFICIENT, dB/km/g/m³, at 20° C

Source	Frequency - GHz									
	15	35	70	95	150	300	1000	2000	3000	3000
Koester & Kowsowsky ^{4,5}		0.55	2.03	3.4						
Kerr ⁷	0.112	(30)0.44	1.35	3.4	7.14					
Chu & Hogg ²¹		0.4	2	3.2	7	14.5	45	70	100	100
Dudzinsky ²²	0.12	0.5	2.05	3.6	7.4	15				
Wilcox ²³	0.23	0.45	2.5	4.1	8	15	46	70	100	100
Rogers ²⁴	0.15	0.63	2.1	3.6	7.5	13				
Best-Fit-Curve	0.12	0.55	2	3.3	7.0	15	45.5	70	100	100

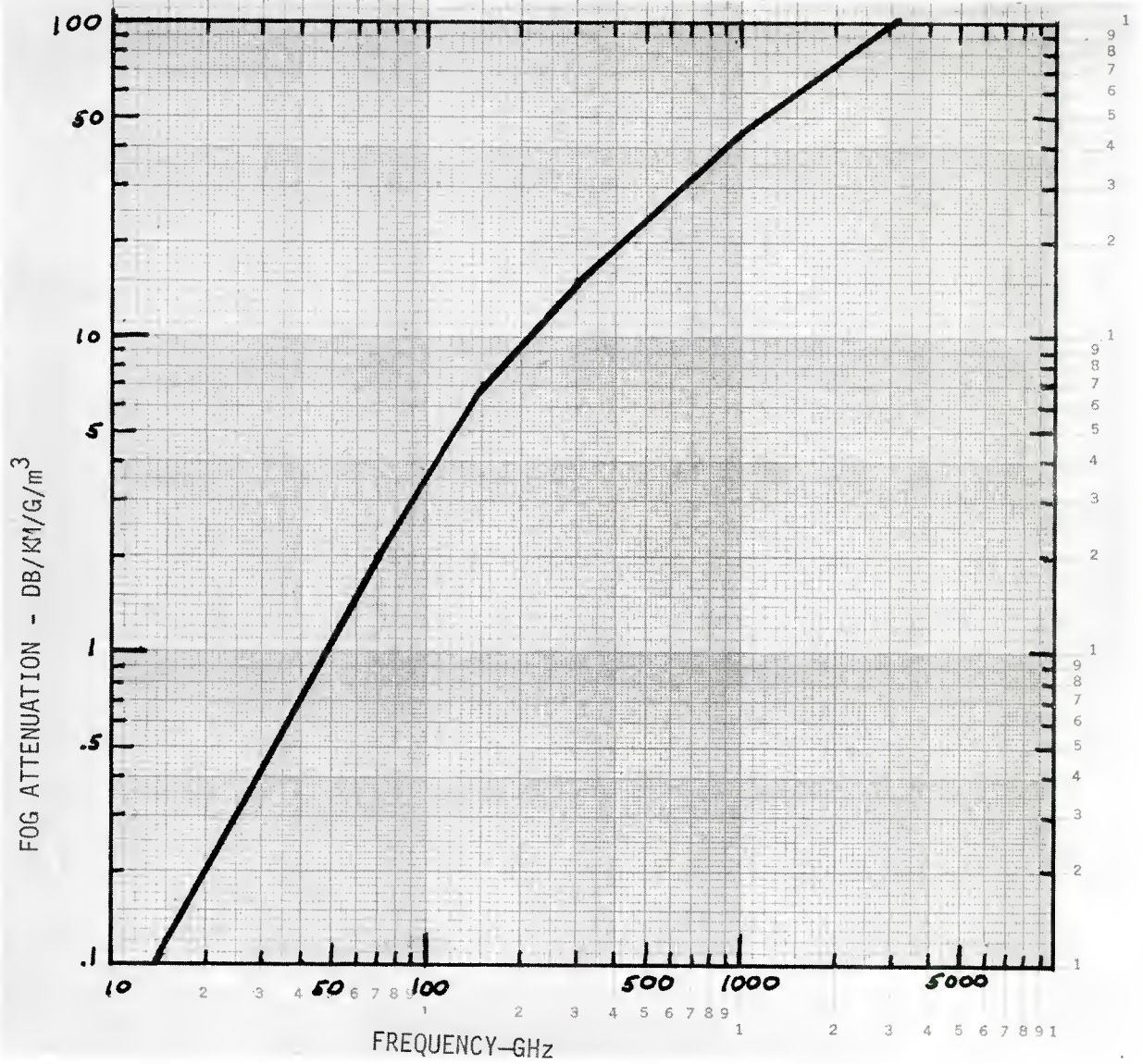


Figure 12. Calculated Fog Attenuation Versus Frequency

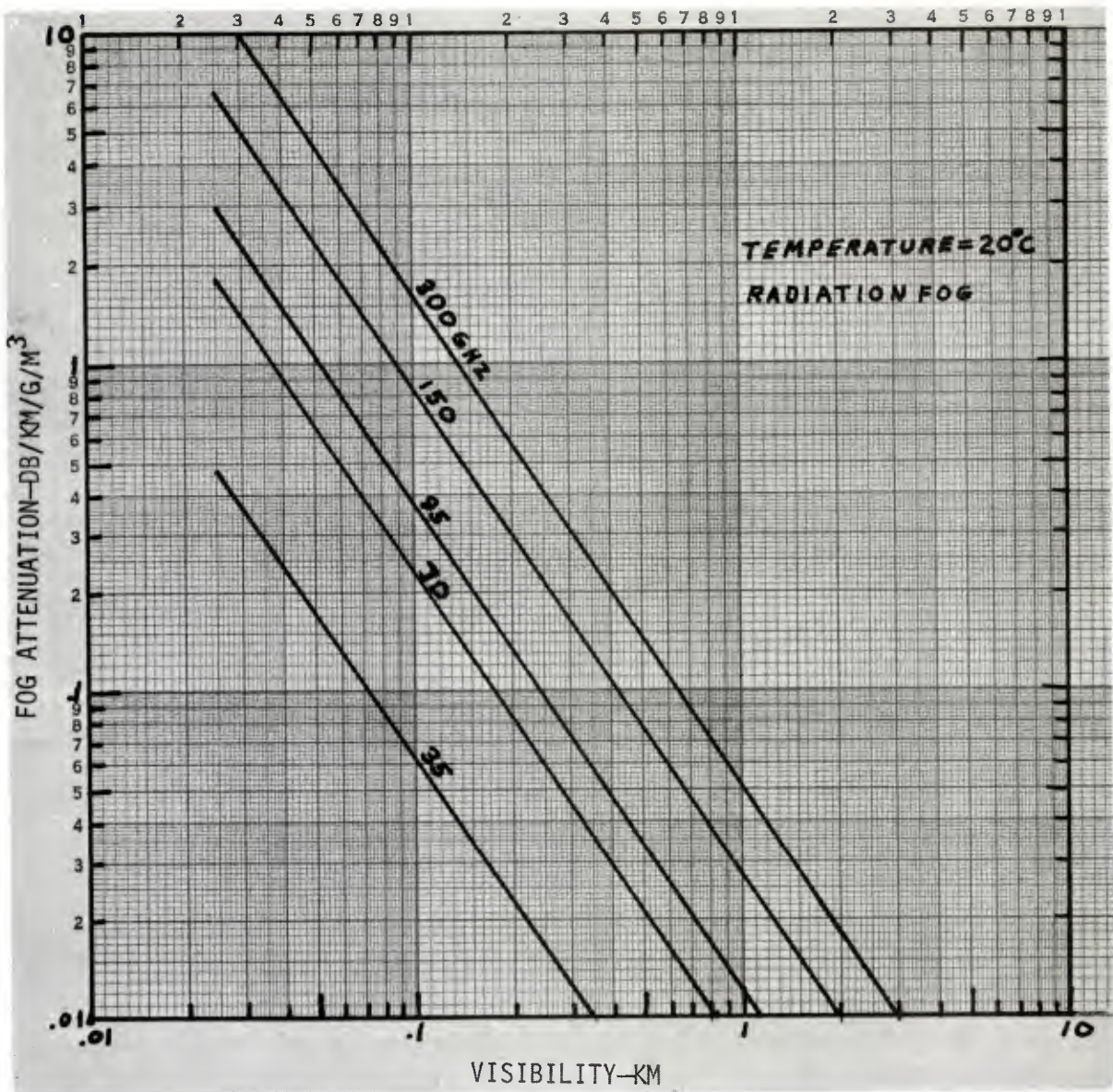


Figure 13. Calculated Fog Attenuation Versus Visibility

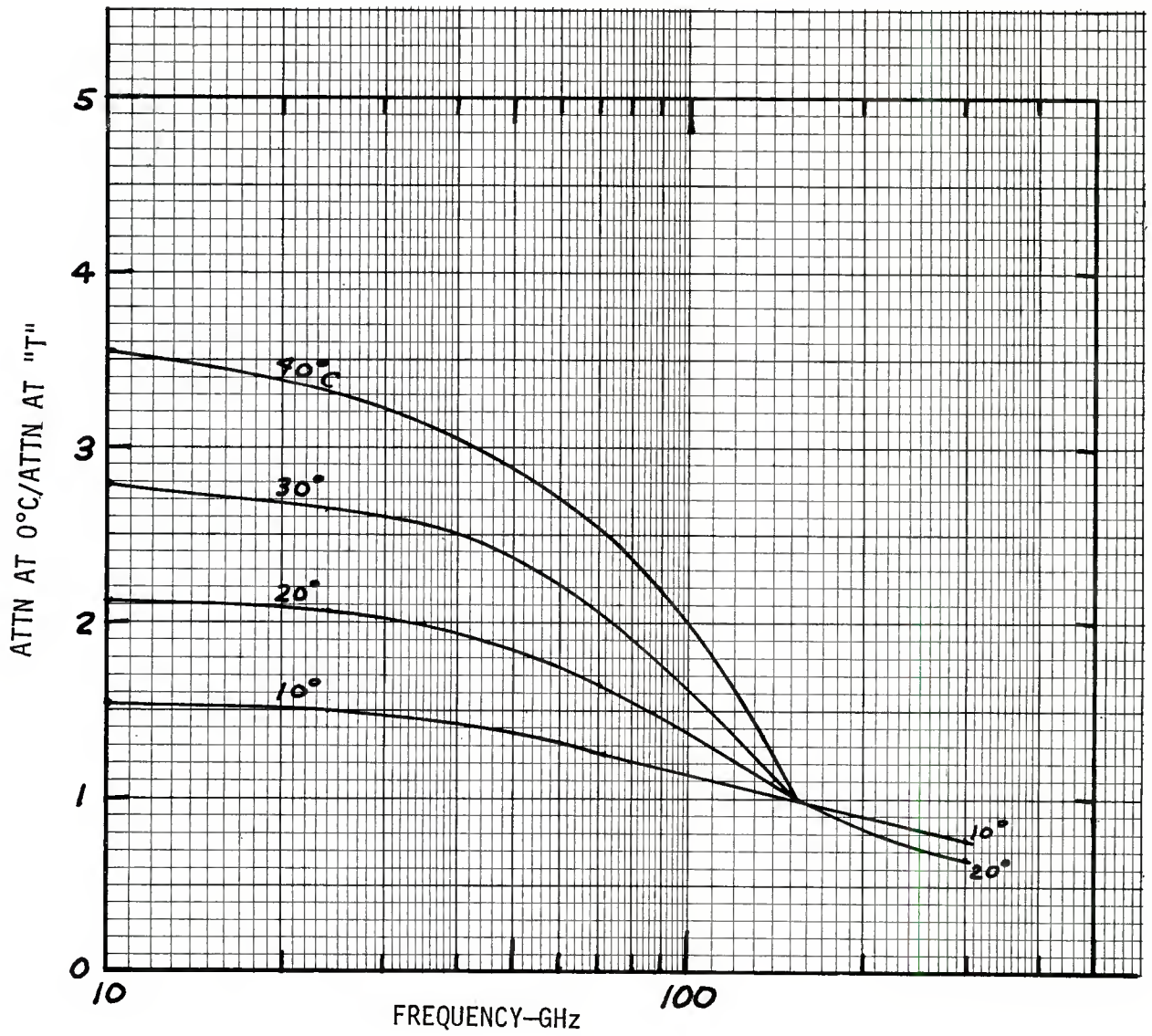


Figure 14. Ratio of Fog Attenuation at T° to Attenuation at 0° C Versus Frequency

low frequencies and diminishes to unity at about 150 GHz, beyond which the attenuation decreases with increasing temperature.

Fog attenuation, in dB/km/g/m³, versus temperature is shown in Figure 15 for frequencies between 15 and 300 GHz. The reduced effect of temperature on attenuation as the frequency increases can be seen in this figure. Above 150 GHz, only two data points were found for 300 GHz which indicate an increase in attenuation with increasing temperature.

Fog attenuation changes with temperature because of the temperature dependence of the relaxation time of the water molecule in equation (16), which enters into equation (15) for the complex dielectric constant of water in the $\Delta\lambda$ term, the transition wavelength or line width. Over the temperature range of 0° to 40° C, $\Delta\lambda$ changes from 3.59 to 0.857 cm, as measured by Saxton and Lane.¹² The temperature effect varies with frequency because of the term $\Delta\lambda/\lambda$ in equation (15).

B. Rain Attenuation and Visibility

1. Rain Measurements. Visibility and 140 GHz attenuation measurements were made during nine rain storms. They were typically long duration rains with slow changes in rainfall rate, which was very desirable for making accurate attenuation and rainfall rate measurements. Although rain cells smaller than the propagation path length did exist occasionally and care had to be exercised to use data only during periods of uniform rainfall rate as indicated by the three rain gauges.

A complete plot of all of the data points from the nine rain storms is shown in Figure 16. The equation of the least squares fit curve is

$$\alpha_r = 1.2 R^{0.75} \quad (17)$$

where α_r is rain attenuation in dB/km and R is the rainfall rate in mm/hr. The scatter of the data points is rather small considering that data are included from nine different rain storms over a period of three months. No significant differences were observed between the attenuation data from the different rain storms. The small scatter of the data is a result of the care exercised in selecting data readout times only when the received signal level was relatively constant and the three rain gauges indicated nearly equal rainfall rates. Even over the relatively short path length of 725 metres, differences between the gauges of as much as four to one were sometimes observed. Preliminary data reduction efforts with less care in selecting readout times resulted in extremely wide data scatter.

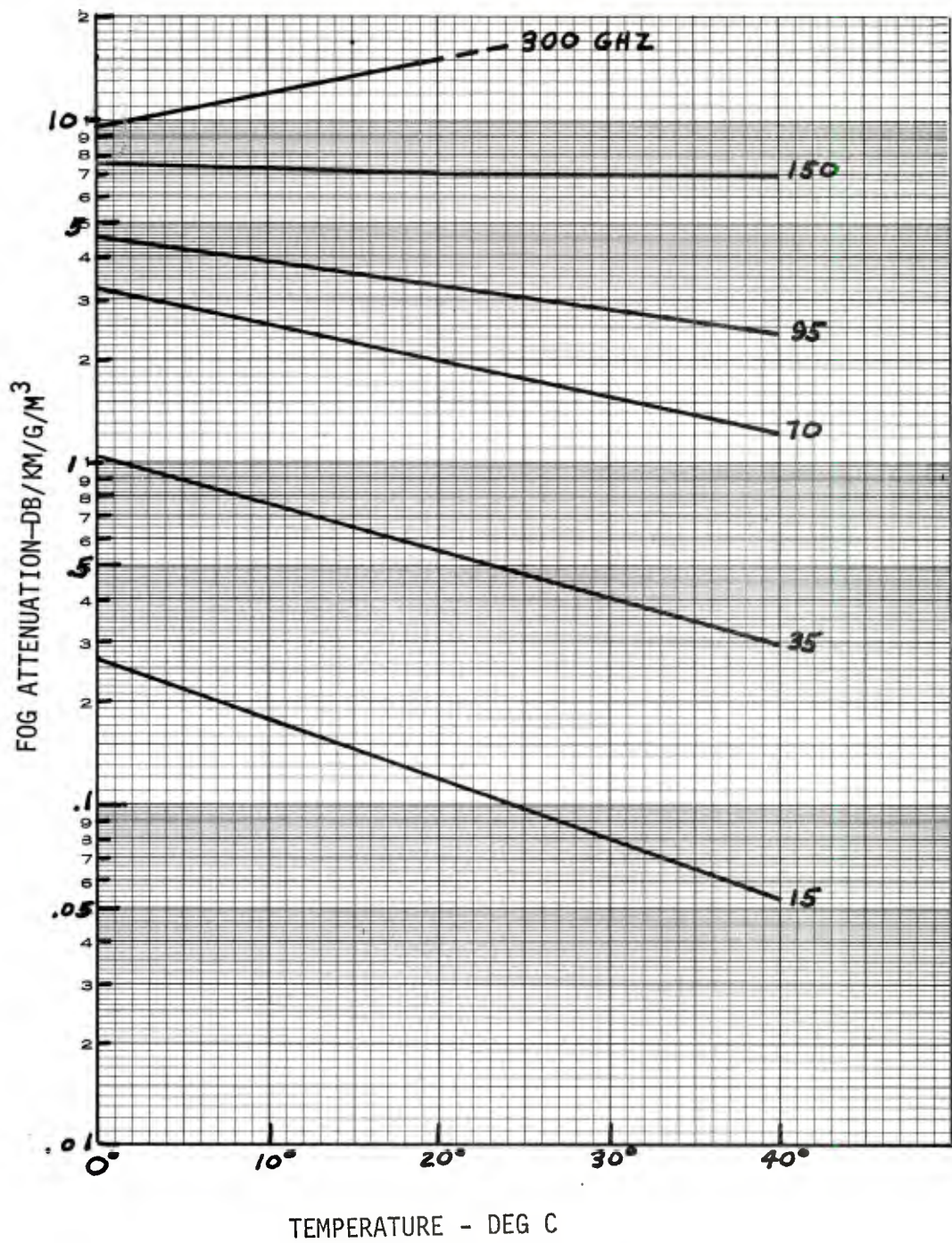


Figure 15. Fog Attenuation Coefficient Versus Temperature

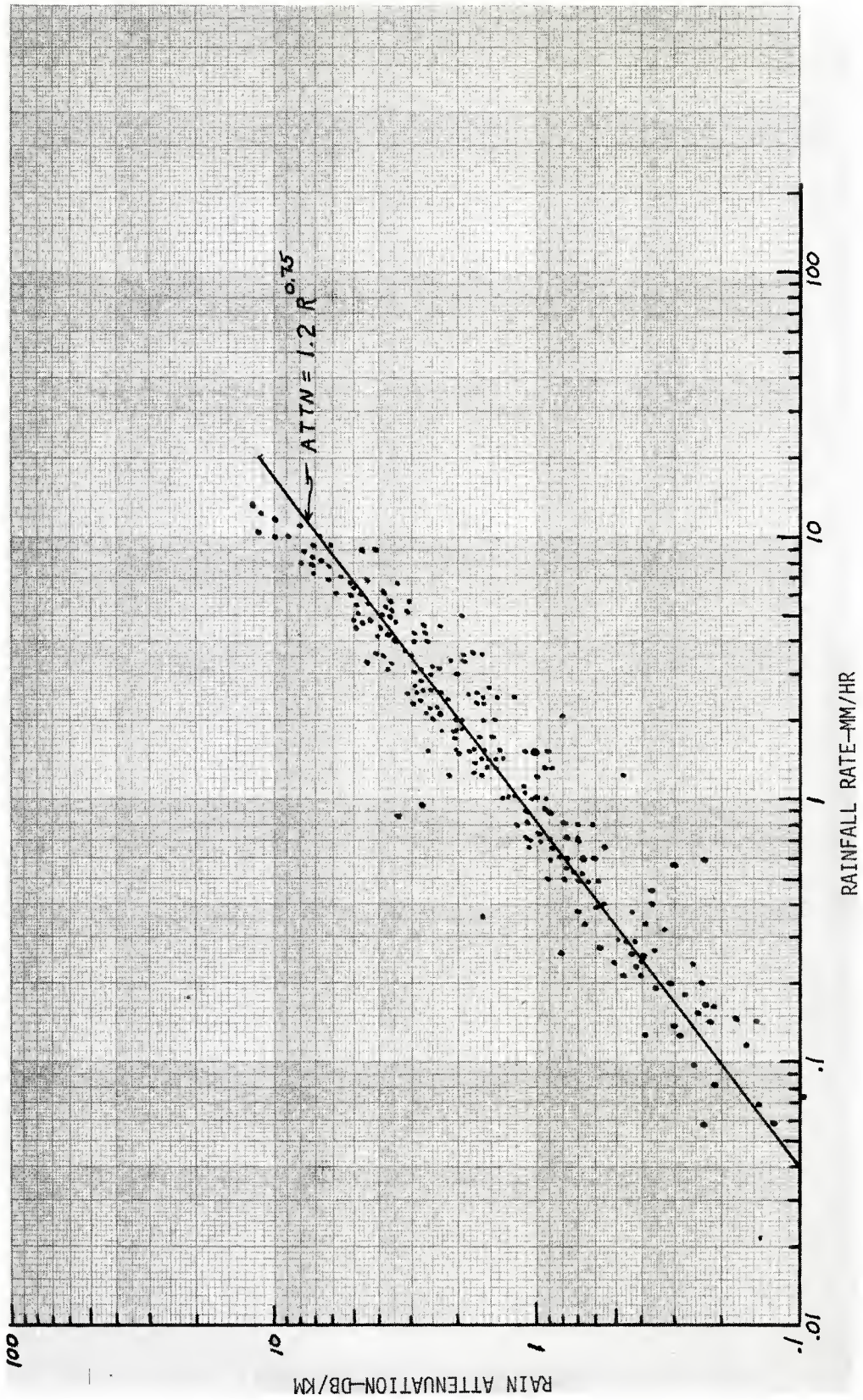


Figure 16. Measured One-Way Attenuation 140 GHz Versus Rainfall Rate

A problem was encountered during the experiment with rain falling on the lucite window in front of the receiving antenna and causing a large and variable attenuation. A comparison of rain attenuation measured with and without a lucite window exposed to rain disclosed that the wetted window introduced significant attenuation that varied with the rainfall rate. The results of this comparison are shown in Figure 17. The window was a flat, vertical sheet of 1/8-inch thick lucite that was mounted flush with the outer surface of the instrument trailer housing the receiving antenna. The slight decrease in attenuation above 10 mm/hr in Figure 17 could be caused by the thickness of the water layer on the window approaching a multiple of one-half wavelength where the reflection losses are reduced or it could be due to the rapid runoff of the water on the vertical window. At the lower rainfall rates, the water accumulates in the form of drops adhering to the window.

A test was made to check the 140 GHz attenuation of a thin layer of water on a vertical sheet of lucite. Water was poured over the sheet and the attenuation was measured as the water ran off. Figure 18 shows the record obtained of attenuation versus time. Just after pouring the water, the attenuation reached a maximum of 5 dB, which includes 0.75 dB due to the dry lucite; after about two minutes the attenuation due to water decreased to 0.75 dB. The attenuation returned to the initial dry lucite value after wiping off the water.

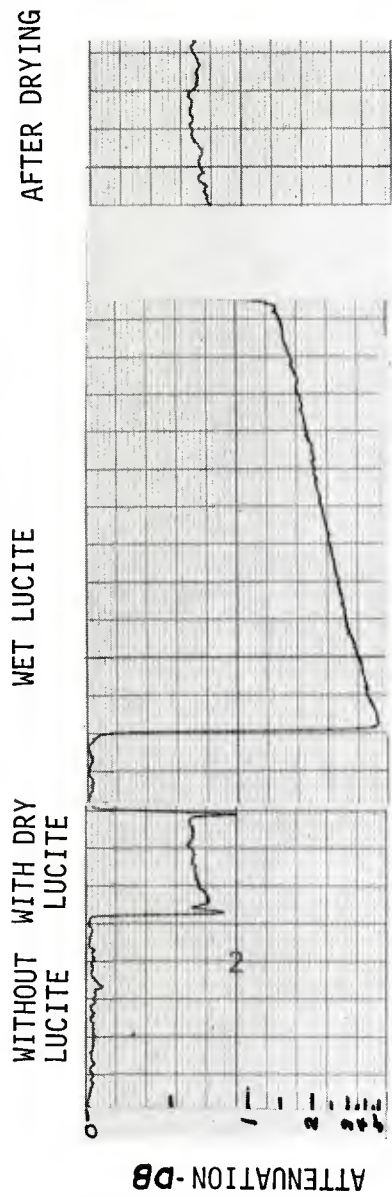
This measurement of a maximum attenuation of 4.25 dB and a calculated attenuation by Chu and Hogg²¹ of 4 dB at 140 GHz for a 0.1-mm thick water layer agrees reasonably well with the measurement during rain of 3.5 dB maximum attenuation due to the wetted window.

Other rain attenuation measurements at 140-150 GHz have been reported by Tolbert, et al²⁵ and Sander.^{26,27} Figure 19 shows measured data points by Tolbert, and regression curves of Sander's and BRL measured data, along with a curve of calculated attenuation by Tolbert. The agreement between the Sander, BRL, and calculated curve is excellent. The Tolbert measured data points for two of the days also fall close to the other curves, but some of the data from 5 May 1954 are

²⁵Tolbert, C.W., Gerhardt, J.R., and Bahn, W.W., "Rainfall Attenuation of 2.15 mm Radio Wavelength," EERL Rpt 109, Univ. of Texas, Austin, TX, 12 June 1959.

²⁶Sander, J., "Research on the Attenuation of Electromagnetic Waves by Rain with 52, 90.8, and 150 GHz," Doctoral Engineering Dissertation, Tech. Univ., Berlin, D83. Translation, USA Foreign Science & Technology Center, FSTC-HT-23-299-75, DIA Task No. T741801, 27 Mar 1975.

²⁷Sander, J., "Rain Attenuation of Millimetre Waves at $\lambda = 5.77, 3.3,$ and 2 mm," IEEE Trans. Ant. & Prop., AP-23, 2, 213-220, Mar 1975.



ATTENUATION DECREASING AS WATER RUNS OFF

Figure 18. Measured Attenuation of Wetted Lucite Window

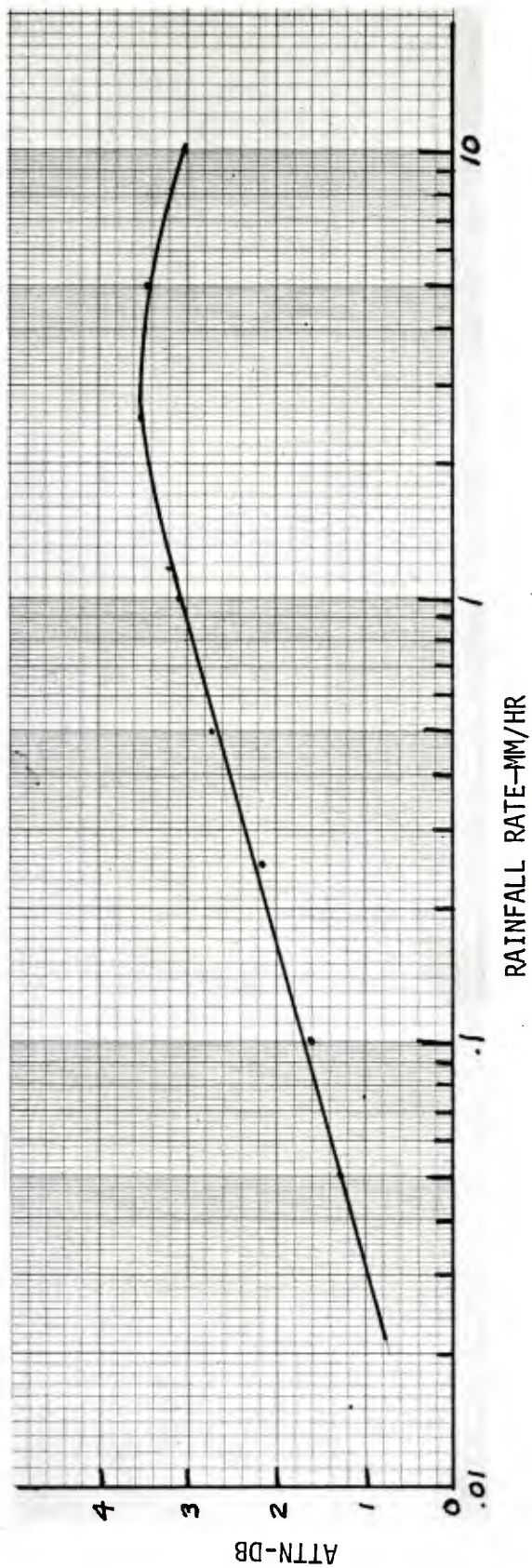


Figure 17. Measured Attenuation of Lucite Window Versus Rainfall Rate

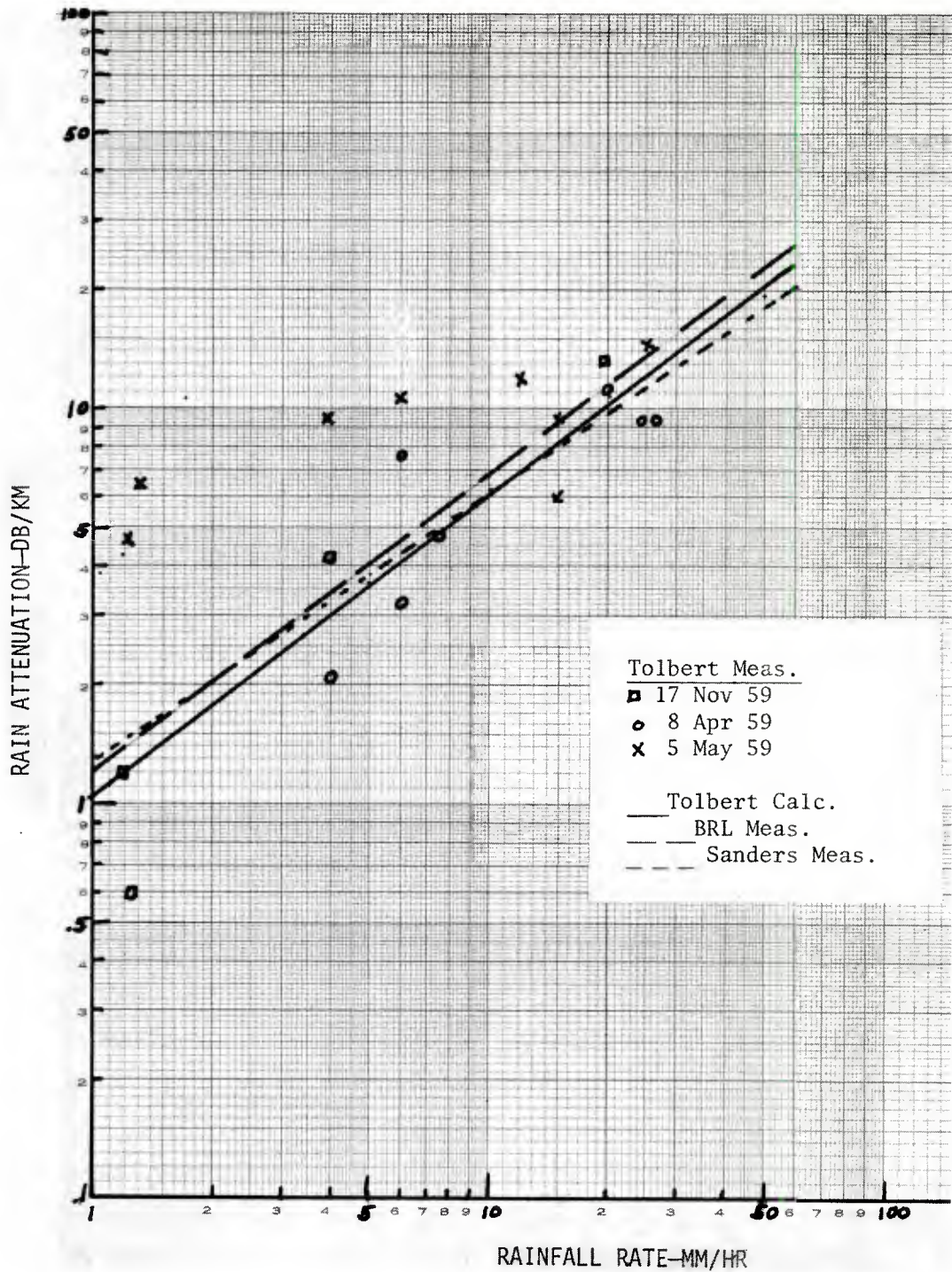


Figure 19. Measured and Calculated Rain Attenuation by Tolbert, Sanders and BRL

considerably higher, although this is not unusual for rain attenuation data. For rain attenuation measurements to be statistically significant, a very large number of readings are required because of the large possible variability of raindrop-sizes and rainfall rate along the propagation path. All of Tolbert's data points are within the peak-to-peak scatter of Sander's data which includes over a thousand data points between 0.2 and 20 mm/hr.

2. Rain Attenuation Calculation. A number of theoretical studies of rain attenuation covering 140 GHz have been reported in which the effects of factors such as drop-size distribution, raindrop shape, complex refractive index of water, temperature, fall-velocity of raindrops, relative forward scattering and absorption, and dispersive properties of rain have been investigated.

Figure 20 shows calculated 140 GHz rain attenuation data by several authors that have been selected to illustrate the magnitude of the difference between calculated values when different drop-size distribution functions are used. The data by Zuffrey²⁸ are based on the Laws and Parsons²⁹ drop-size distribution which is an empirically derived, Rayleigh-shaped curve with peak numbers of drops occurring at larger drop sizes as the rain intensity increases. Debye's formula for the complex dielectric constant of water and Saxton and Lane's¹² constants were used. Zuffrey's report contains a very thorough analysis of the effects of rain on propagation between 1 and 600 GHz. Included are computations of the effects of temperature, drop-size distribution function, and raindrop fall-velocity. Propagation conditions under which multiple scatter effects can be neglected are given. The dispersive properties of rain are discussed, including the effect of the variation in propagation time delay as a function of frequency on the signal delay distortion and bandwidth. The accuracy of the Debye model for computing the complex refractive index of water is evaluated. A computer program is included for the calculation of rain attenuation.

The data in Figure 20 by Sander^{26,27} are based on the Marshall and Palmer³⁰ drop-size distribution, which is a negative exponential shaped function. This distribution heavily emphasizes the number of small

²⁸Zuffrey, C.H., "A Study of Rain Effects on Electromagnetic Waves in the 1-600 GHz Range," *Master's Thesis*, Dept. Electrical Engineering, Univ. of Colorado, 1972.

²⁹Laws, O.J. and Parsons, D.A., "The Relation of Raindrop Size to Intensity," *Trans. Am. Geophysical Union*, Vol 24, 452-460, 1943.

³⁰Marshall, J.S. and Palmer, W. McK., "The Distribution of Raindrops With Size," *Jour. of Meteorology*, Vol. 5, 165-166, Aug 1948.

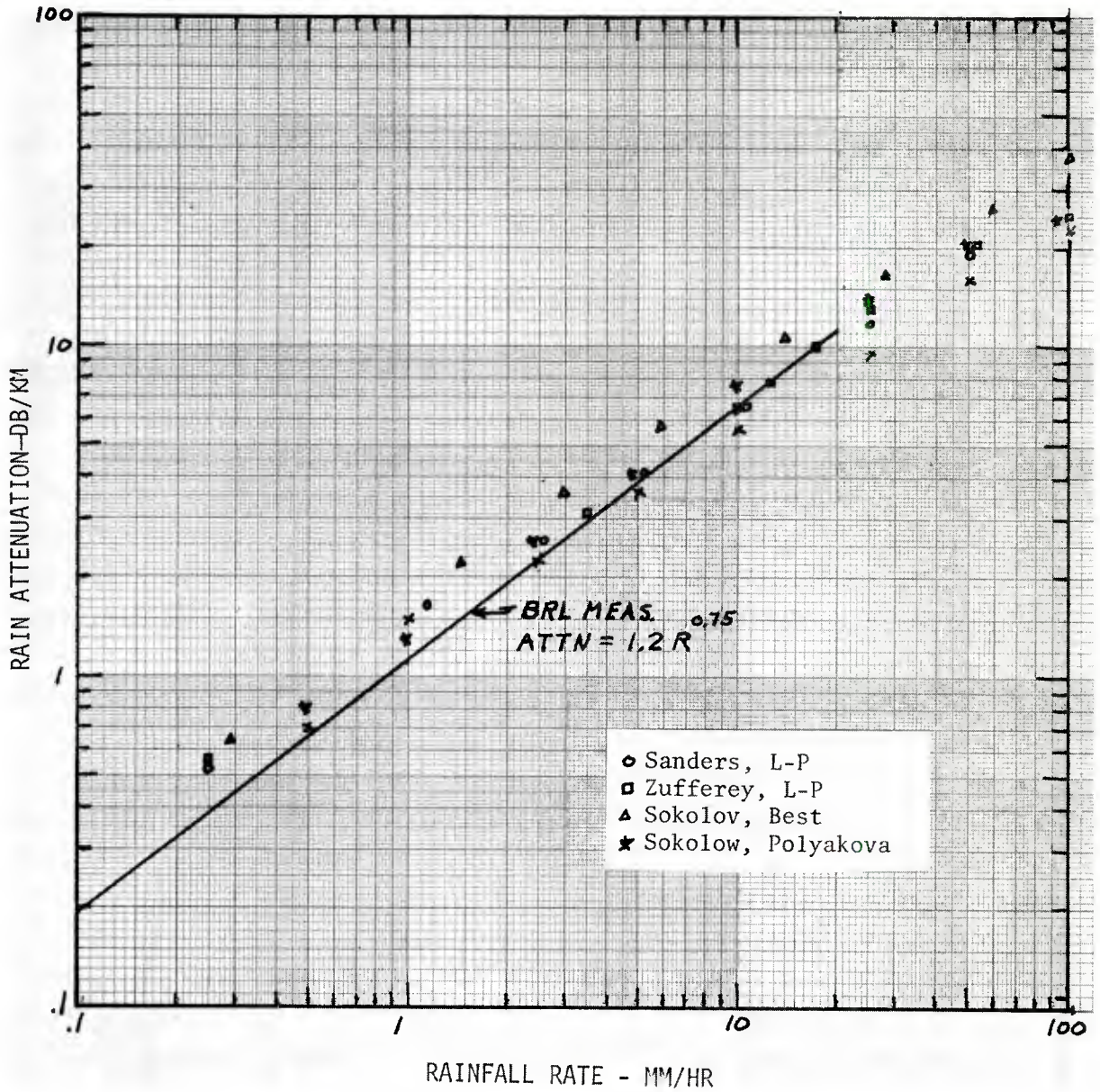


Figure 20. Calculated Rain Attenuation Versus Rainfall Rate

drops and, as can be seen in Figure 20, gives a higher attenuation than other distributions. Sander has conducted an extensive theoretical and experimental investigation of rain attenuation at 52, 90 and 150 GHz. Causes that affect the correlation between measured attenuation and rain intensity are analyzed in depth. Comparisons are made between the Laws and Parsons,²⁹ Marshall and Palmer,³⁰ and Diermendjian^{16,17} drop-size distribution. Sander's rain attenuation calculated using the Laws and Parsons distribution agrees with Zuffreys²⁸ as shown in Figure 20. Attenuation coefficients calculated for deformed raindrops are reported to scarcely differ from spherical drops at 150 GHz because the rain contribution to attenuation is from the small raindrops that do not deform appreciably while falling. Also, the magnitude of forward scattering is found to be negligible at 150 GHz. The characteristics and limitations of rain collecting and drop-size measuring instruments are reviewed, including a very complete error analysis. A fast-response electrostatic type of drop-size measuring instrument was used called the rain analyzer, which is described by Lammers.³¹ The interesting possibility of the use of the ratio of rain attenuation coefficients measured at several frequencies to describe the drop-size distribution is discussed. Sander's calculated attenuation data for 50, 90.2 and 150 GHz are tabulated for 0°, 10° and 180° C and nine rainfall rates between 0.25 and 150 mm/hr in Reference 26.

Setzer³² has calculated rain attenuation for thirteen frequencies between 1.43 and 300 GHz, including 150 GHz, at rainfall rates from 0.25 to 150 mm/hr. The Laws and Parsons²⁹ distribution was used. The results are tabulated in terms of the scattering coefficient, absorption coefficient, extinction coefficient and the complex index of refraction of water. Rain attenuation in dB/km is 4.343 times the extinction coefficient. Setzer's rain attenuation values agree with those of Sander^{26,27} and Zuffrey²⁸ at 150 GHz also based on the Laws and Parsons distribution.

Tolbert et al²⁸ demonstrate that at 140 GHz the calculation of rain attenuation using on-site measurements of the drop-size distribution improved the relationship between measured and calculated attenuation over a short time period. The inhomogeneity of the rainfall along the path and the difficulty of determining the applicable drop-size distribution were considered to be responsible for the large part of the discrepancy they often observed between measured and calculated rain attenuation.

³¹Lammers, U.H.W., "Electrostatic Analysis of Raindrop Distributions," *J. Appl. Meteor.*, 8, 3, 330-334, 1969.

³²Setzer, D.E., "Computed Transmission Through Rain at Microwave and Visible Frequencies," *BSTJ*, 49, p 1873, 1970.

Several articles in the Russian open literature have been published on theoretical studies of rain attenuation covering 150 GHz and based on the conventional Laws and Parsons and Marshall and Palmer drop-size distribution as well as several others not commonly used by U.S. authors. Data by Sokolov and Sukhonin³³ are shown in Figure 20 based on a drop-size distribution empirically derived by Polakova³⁴ from measurements in Russia. There is good agreement between these data and the previous author's calculations using the Laws and Parson's distribution.

Rozenberg³⁵ reports on rain attenuation calculations for frequencies from 3 to 1000 Ghz using drop-size distributions by Marshall and Palmer,²⁰ and Best.³⁶ The results using Best are lower by about 15% at low and medium rainfall rates and lower by 30% at heavy rainfall rates compared with calculations based on the Laws and Parsons distribution. Rozenberg is the only author known to investigate in some detail the attenuation of drizzle at 150 GHz. His calculations using several drizzle drop-size distributions give attenuation values between 0.05 and 0.15 dB/km for intensities of 0.1 mm/hr. The attenuation of rain with drizzle at a rainfall rate of 1 mm/hr is shown to be about 1.1 dB/km which agrees with Figure 19. Thus, even though drizzle has a predominance of small drops, the attenuation is shown to be about the same as for rain.

Naumov and Stankevich³⁷ have also calculated rain attenuation, covering the frequency range of 60 to 600 GHz. Their article is not clear whether the Marshall and Palmer or the Best distribution is used; both are referenced.

3. Temperature Effect on Rain Attenuation. The temperature effect on rain attenuation is very small at 150 GHz. The effect is largest at

³³Sokolov, A.V. and Sukhonin, Ye. V., "Attenuation of Submillimetre Radio Waves in Rain," Radio Eng. and Elec. Phys., 15, 12, 2167-2171, Dec 1970.

³⁴Polakova, Ye. A., "Investigation of the Microstructure of Rains in Connection with the Question of Their Transparency," Trans. (Trudy GCO), Proc. of the Main Geophysical Observatory, Issue 220, Chap 2, Sec. 4, (Gidrometecizdet) 1967.

³⁵Rozenberg, V.I., "Radar Characteristics of Rain in Submillimetre Range," Radio Eng. & Elec. Phys., 15, 12, 2157-2163, Dec 1970.

³⁶Best, A.C., "The Size Distribution of Raindrops," Quart. J. Roy. Meteor. Soc., 76, 16-36, 1950.

³⁷Naumov, A. D. and Stankovich, V.S., "On the Attenuation of Millimetre and Submillimetre Radio Waves in Rain," (Izv. Vuz), Radio Phys. & Quantum Elec., 145-147, Feb 1969.

low rainfall rates. Zuffrey²⁸ calculates a decrease in attenuation of 12% as the temperature drops from 20° to 0° C at 0.25 mm/hr and an increase in attenuation of 3% going from 20° to 40° C. At 25 mm/hr and over, the decrease in attenuation going from 20° to 0° C is 5% and the increase in going from 20° to 40° C is negligible.

4. Wind Effect on Rain Attenuation. The peak-to-peak scatter of measured rain attenuation versus rainfall rate due to wind is very large. Zuffrey²⁸ has shown that peak attenuation values measured often exceed the maximum theoretically possible attenuation assuming zero vertical wind and the rain to be composed entirely of drops of the size that give maximum attenuation for the frequency of interest. Thus, errors in the drop-size distribution function would not explain the large attenuation. In addition, the error in measuring rain intensity would have to be unreasonably large. To explain this phenomenon, Zuffrey calculated rain attenuation assuming a 3 m/sec upward component of wind, a value considered reasonable for medium and heavy rain storms. The attenuation with such a vertical wind is much larger than for the normal, zero wind assumption because there is much more water in the path than collected by the rain gauge. At 150 GHz, the attenuation with a 3 m/sec vertical wind was 16 times greater than for zero vertical wind. The correction factor for the vertical component of fall-velocity of raindrops in the presence of a vertical wind component appears to be much more significant than the effects of drop-size distribution, non-sphericity of drops, and temperature in explaining measured data greatly exceeding the average model.

5. Rain Visibility Measurements. Optical visibility was measured simultaneously with rain attenuation during a rain storm. A composite plot of attenuation as a function of visibility data from six rain storms is shown in Figure 21. The large scatter of the data is an indication of the rather weak relationship between 140 GHz rain attenuation and visibility. This is because 140 GHz attenuation is strongly dependent on the total water **whereas** optical visibility is more strongly affected by the small droplets. Figure 21 is useful for determining limits and average values of attenuation as a function of visibility to be expected in practice since data from six different rain storms are included.

Shown in Figure 22 is a curve of visibility versus rainfall rate that has been derived from the best-fit curves of Figures 16 and 21. It is interesting to compare the visibility of rain and fog for the same liquid content. From Figure 22, the liquid water content of rain at 1.6 mm/hr is 0.1 g/m^3 and the visibility is 5.6 km. From Figure 11, radiation fog at 0.1 g/m^3 has a visibility of only 0.12 km.

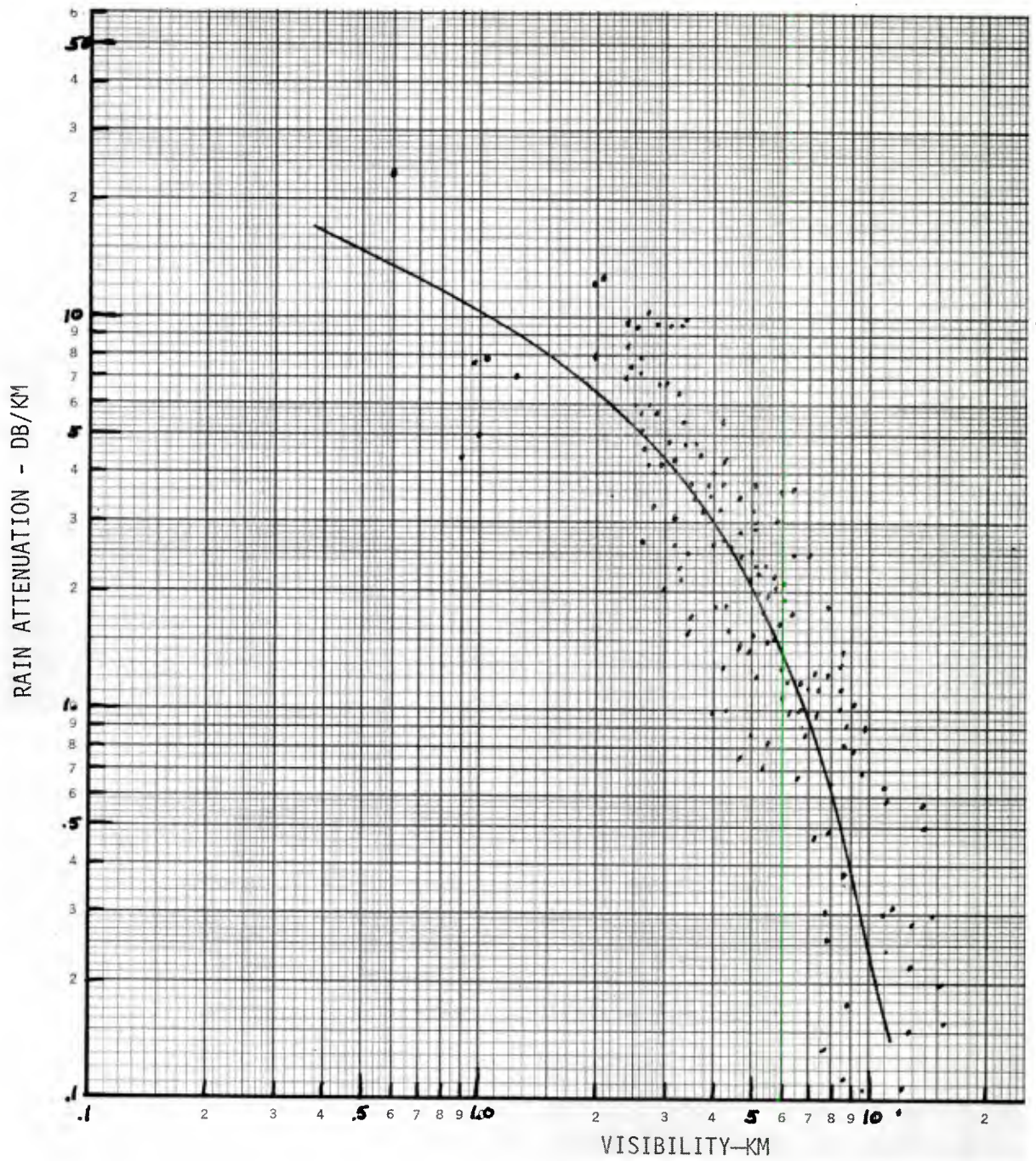


Figure 21. Measured Rain Attenuation Versus Visibility

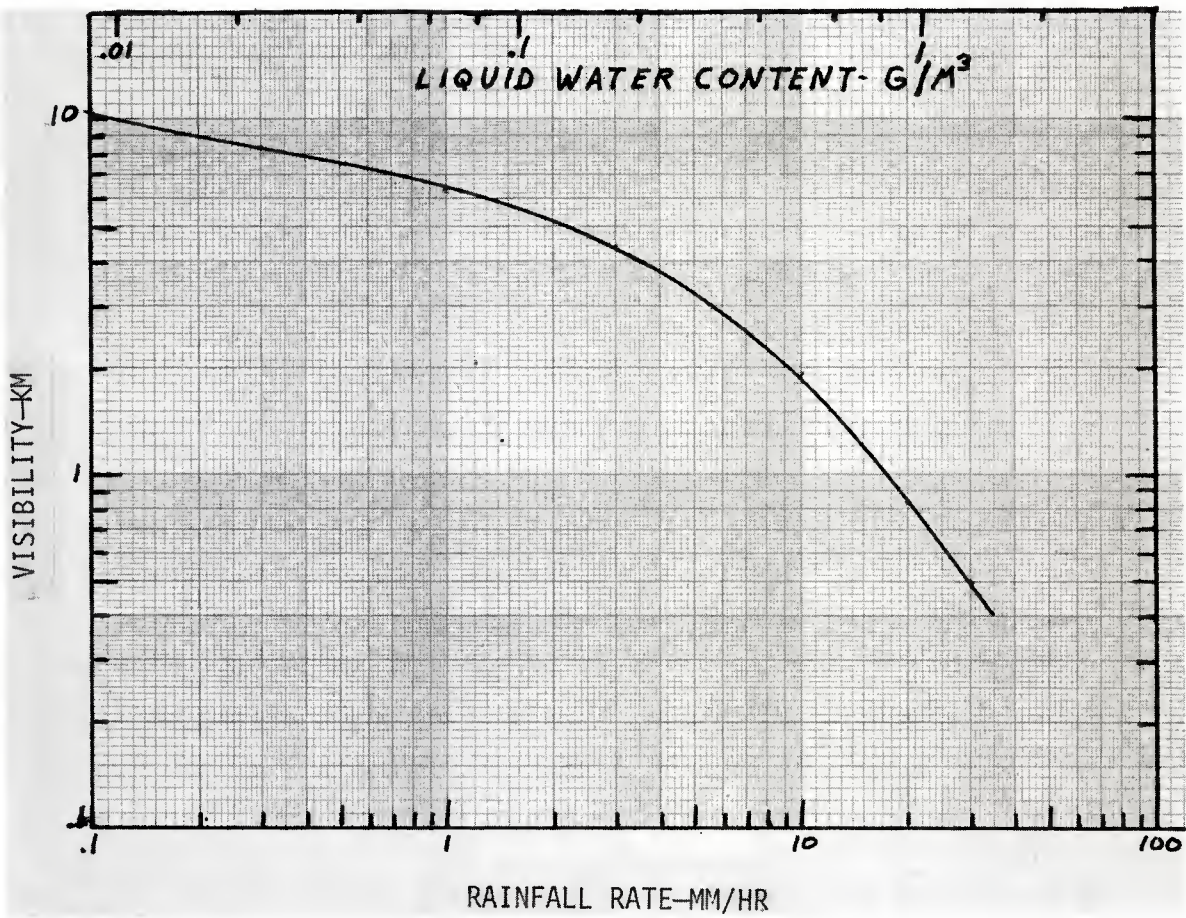


Figure 22. Visibility Versus Rainfall Rate

C. Snow Attenuation and Visibility

1. Snow Measurements. Measurements of attenuation at 140 GHz and optical visibility were made during a three-hour portion of a snow storm characterized by having large, moist snowflakes. A tipping bucket rain gauge with heating elements wrapped around the collector funnel was used to measure the snowfall intensity in terms of the equivalent rainfall rate in mm/hr.

A section of a paper chart record is shown in Figure 23 which illustrates the type of data recordings made and the close correlation between attenuation, visibility and bucket tip rate. As the snowfall intensity increases, indicated by the closer spacing of the bucket tip pulses, the attenuation increases and the visibility decreases.

The attenuation, visibility, equivalent rainfall rate and liquid water content data for the entire three-hour record are shown in Figure 24. During the first hour of the snow storm (13:00-14:00) the visibility decreased from the initial clear weather condition of over 15 km down to 3 km and the attenuation increased to 0.8 dB/km. The water content of the snow during the first hour was below the 0.025 mm/hr measuring threshold of the tipping bucket gauge. Several brief periods of increase in attenuation can be seen to be correlated very well with a visibility decrease.

During the second hour of the snow storm, (14:00-15:00) the attenuation reached a maximum of 4.7 dB/km with a corresponding 1.33 mm/hr equivalent rainfall rate and visibility of 2 km.

During the third hour of the snow storm, (15:00-16:00) a maximum attenuation of 5.5 dB/km was reached, accompanied by an equivalent rainfall 1.2 mm/hr and visibility of only 1.2 km. During the remainder of the record, the attenuation varied between 1.6 and 3.5 dB/km while the equivalent rainfall varied between 1.8 and 2.1 mm/hr. The visibility followed the general trend of the attenuation curve but remained very low, varying between 1.2 and 1.5 km. The visibility during the latter portion of the record was less than for the same equivalent rainfall during the first part of the snow storm, apparently because of a change in the snowflake characteristics or a mixture of fog and snow.

The data from Figure 24 have been replotted in Figure 25 to show the quantitative relationship between visibility, attenuation, and equivalent rainfall rate. There is a well-defined relationship between attenuation and visibility with respect to equivalent rainfall rate for all but the last portion of record, where evidently there was a change in the characteristics of the storm which reduced the visibility and the attenuation. The equation of the best-fit line through the visibility data points in Figure 25 is

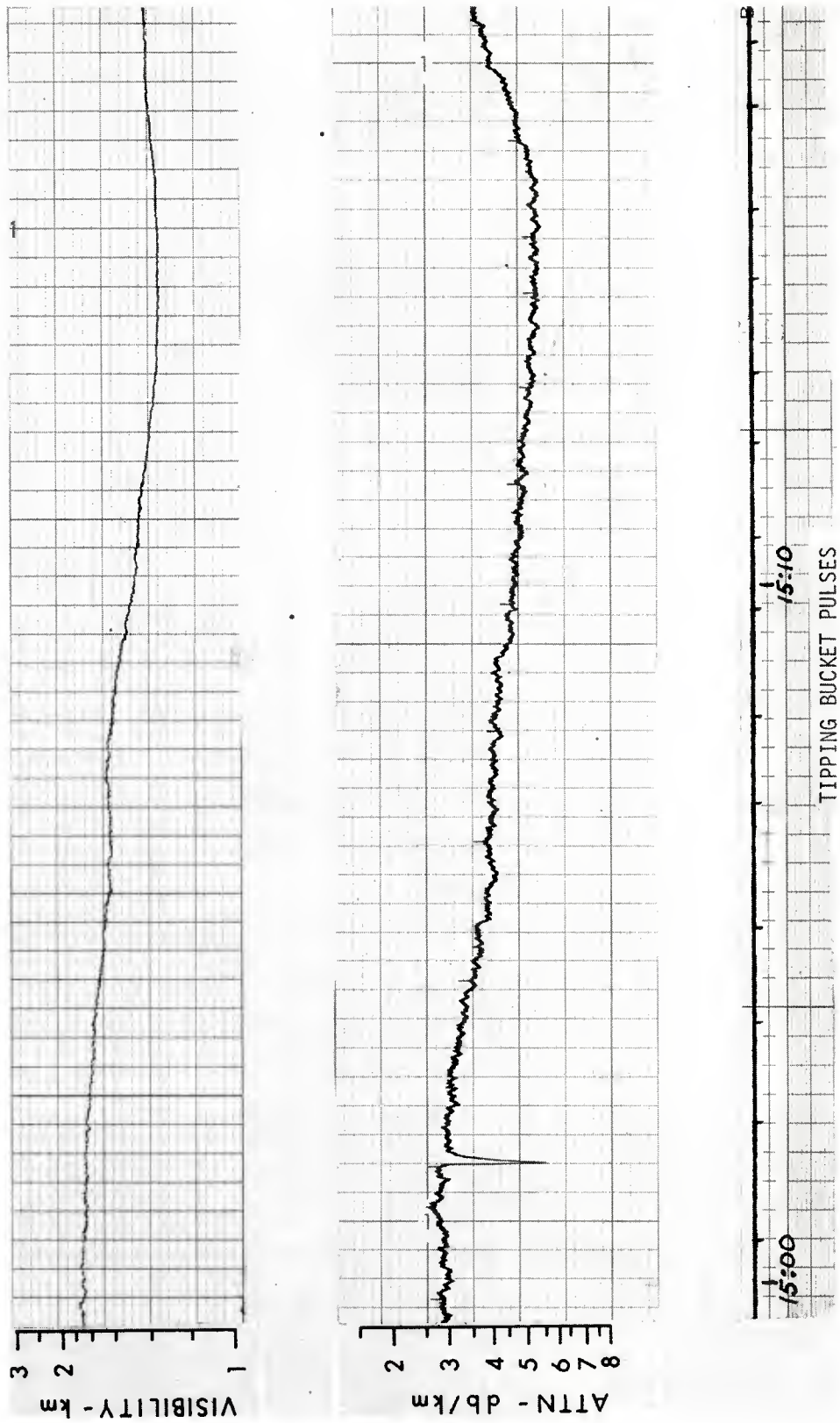


Figure 23. Chart Record of 140 GHz Attenuation, Visibility and Tipping Bucket Pulses During Snow Storm

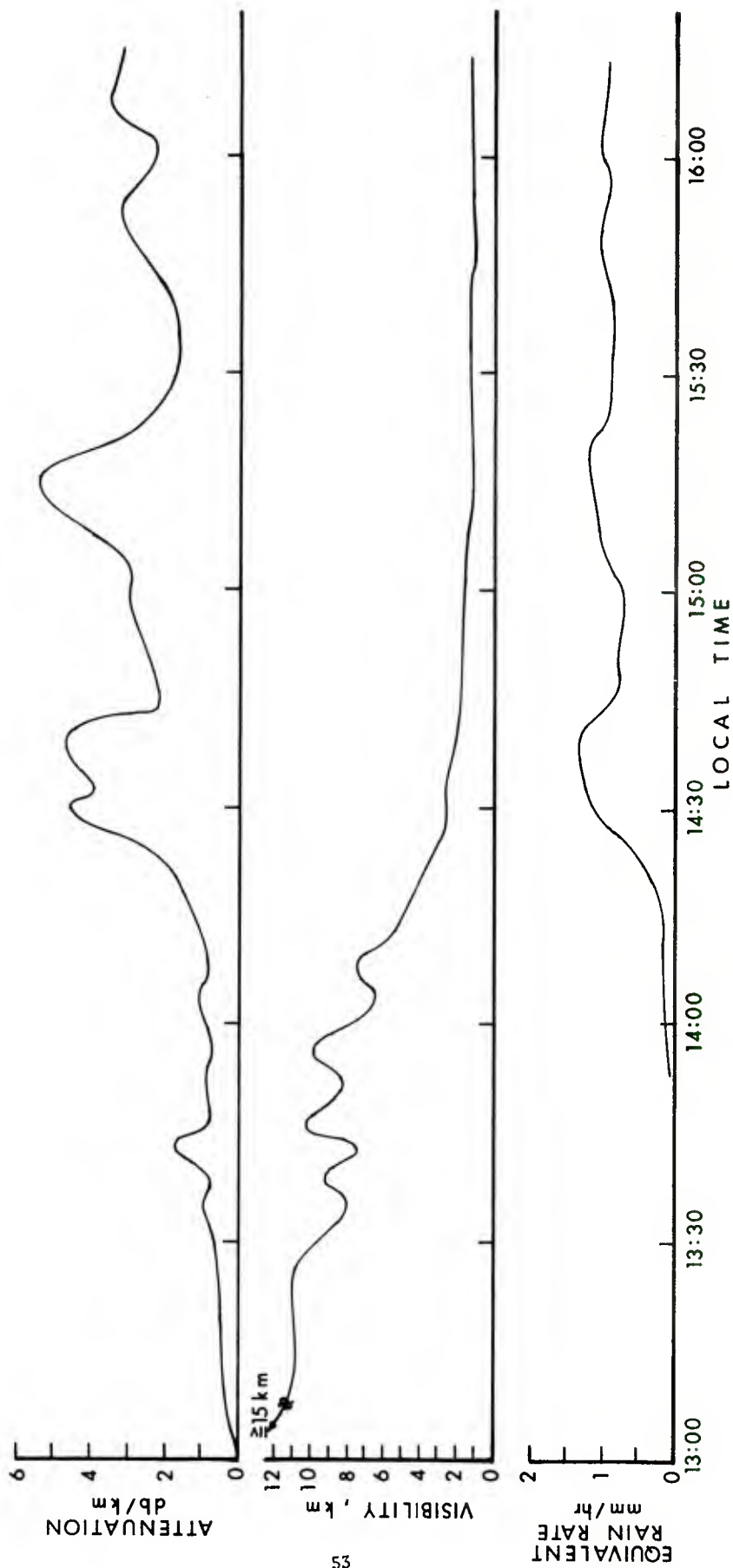


Figure 24. 140 GHz Attenuation, Visibility and Equivalent Rainfall Rate Versus Time

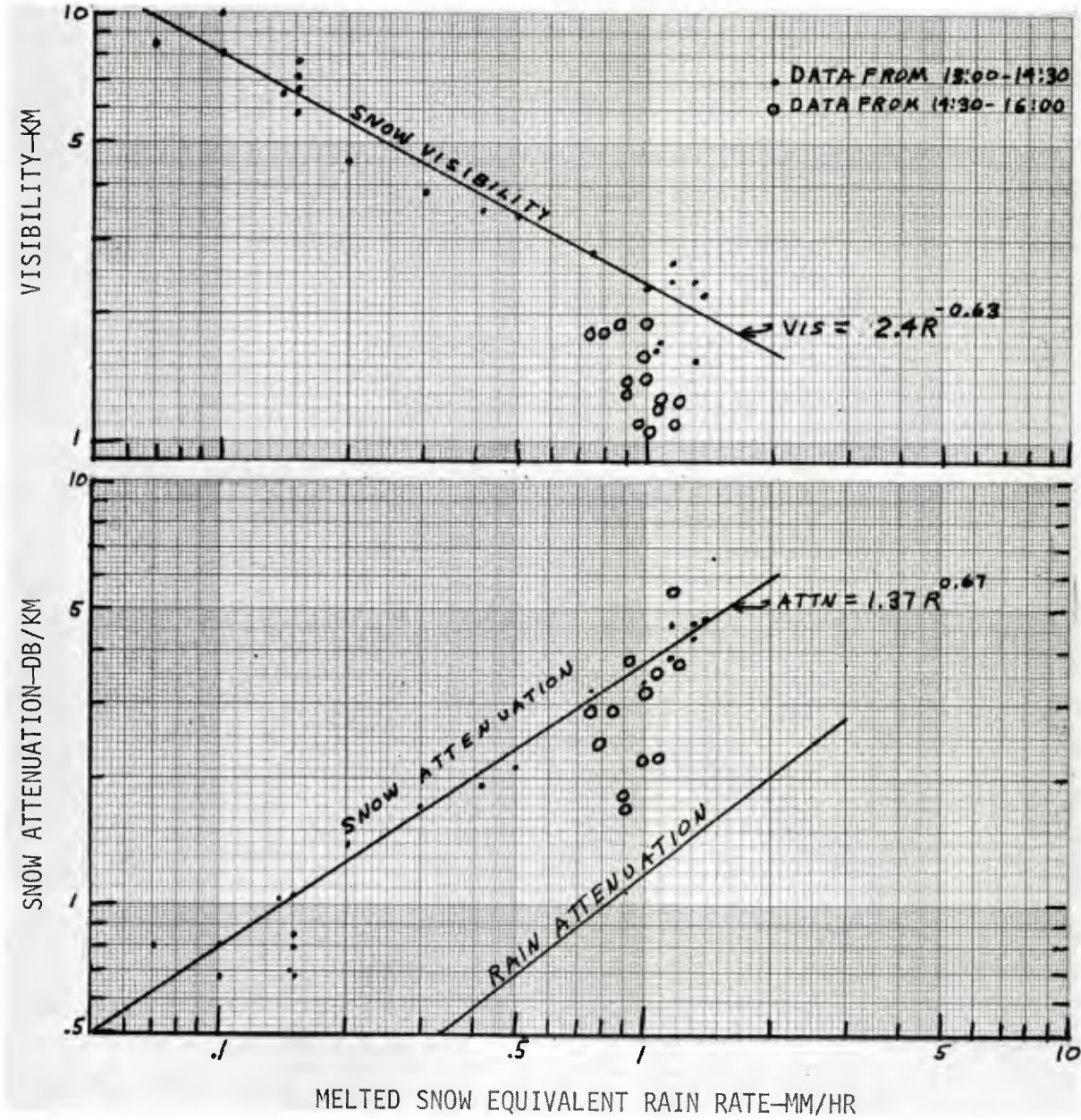


Figure 25. 140 GHz Snow Attenuation and Visibility Versus Melted Snow Equivalent Rainfall Rate

$$V_s = 2.4 R_s^{-0.63} \quad (18)$$

where V_s is the visibility in wet snow, and R_s is the melted snow equivalent rainfall rate in mm/hr.

The equation for the attenuation best-fit line in Figure 25 is

$$\alpha_s = 1.37 R_s^{0.67} \quad (19)$$

where α_s is the attenuation of wet snow in dB/km.

The data for visibility and attenuation in Figure 25 have been re-plotted in Figure 26 as attenuation versus visibility. The equation for this curve is

$$\alpha_s = 11 V_s^{-1.23} \quad (20)$$

A rain attenuation curve is included in Figure 25 for comparison with snow attenuation at the same rainfall rate. The snow attenuation is about three times greater than rain attenuation. The attenuation in moist snow is greater than in rain for the same rainfall rate because of the higher concentration of **snowflakes** as a result of their lower fall velocity. In addition, the larger dimensions and irregular shapes of **snowflakes** compared with raindrops cause greater attenuation.

No other measured or calculated 140 GHz snow attenuation data were found for comparison but some moist snow attenuation measurements have been reported for 35 GHz by Robison,² for 53 GHz by Lammers,^{38,39} 312.5

³⁸Lammers, U., "Investigations on the Effects of Precipitation on MM-Wave Propagation," *Doctoral-Engineering Dissertation, Tech. Univ., Berlin, D83, 1965. Translation by US Army Foreign Science and Technology Center, FSTC-HT-23-0298-75, DIA Task No. T741801, 1975.*

³⁹Lammers, U., "The Attenuation of MM-Waves by Meteorological Precipitation," *Nachr. Techn. Z., 19, 1956 and NTZ-Commun. Journ., 16, No. 5-6, 1967.*

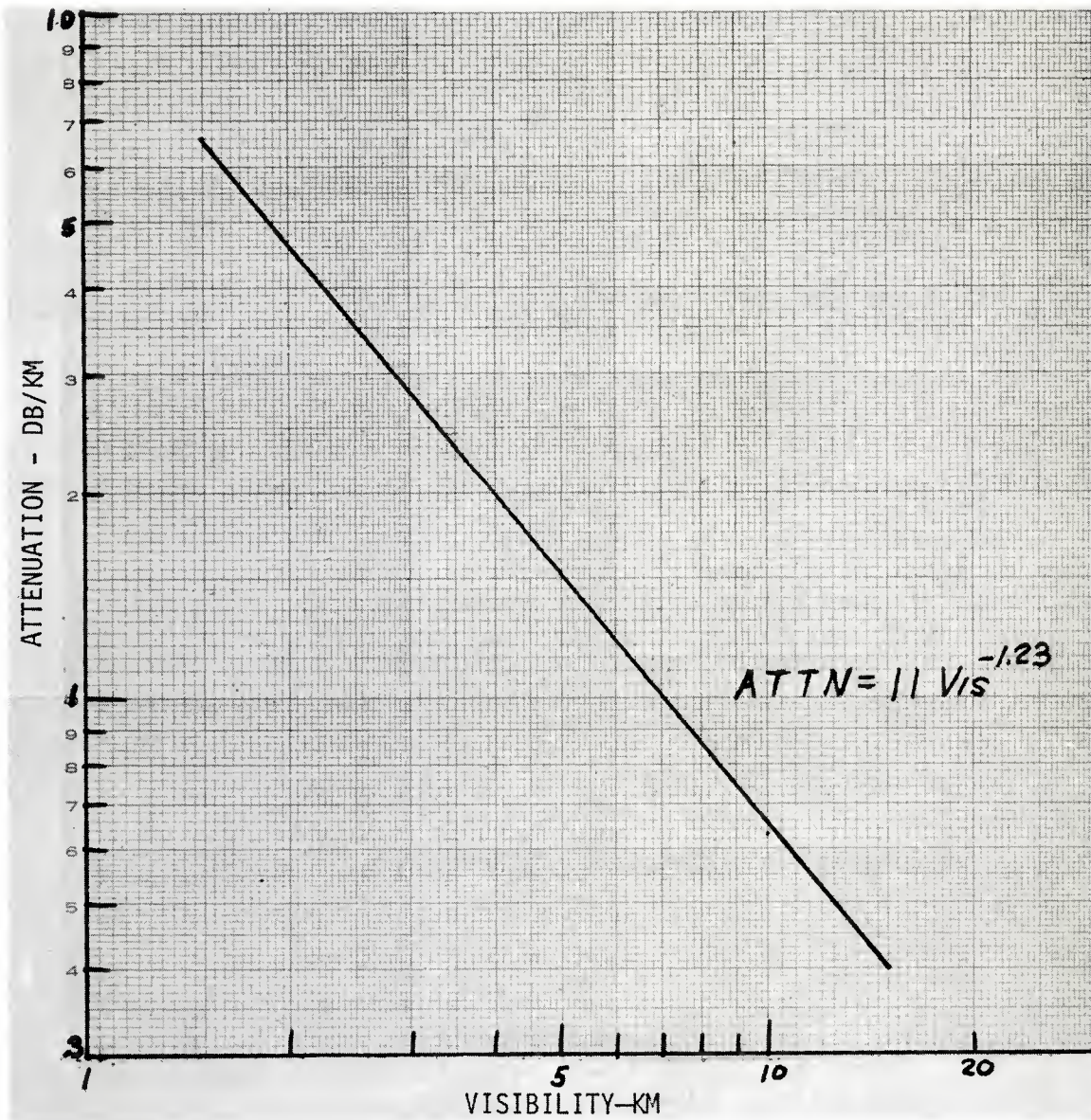


Figure 26. Wet Snow 140 GHz Attenuation Versus Visibility

GHz by Babkin et al.,⁴⁰ and at 0.6 and 10 microns wavelength by Sokolov.⁴¹ Data from these references are shown in Figure 27 for a 1 mm/hr rainfall rate along with a rain attenuation curve. Snow attenuation is between 2.5 and 5 times greater than rain attenuation for all of the frequencies measured. Lammers^{38,39} reports that the measured attenuation of very dry snow at 53 GHz is only 1/6 the attenuation of rain.

The attenuation of snow is very strongly dependent on the moisture state of the snowflakes. When it is very cold and the snow is dry, the attenuation will be very low, less than an equivalent rain attenuation, but, when the temperature is just at the freezing point or above, the attenuation can be much larger than for an equivalent rainfall.

2. Snow Attenuation Calculation. An exact theoretical solution for calculating snow attenuation is difficult to develop because of the complex and diverse shapes of snowflakes and the difficulty of obtaining the index of refraction of real snowflakes with their widely varying ice-air-water composition ratios. Some approximate methods of computation of snow attenuation have been used assuming that snowflakes are spherical with sizes equal to that of water spheres formed by melted snowflakes. The complex index of refraction is defined as that of a mixture of ice and air, (and water if the snow is thawing). The intensity of snowfall is measured by the equivalent melted snow rainfall rate. The calculated attenuation based on these approximations has generally been much lower than measured. A discussion follows on the work of several authors who have reported on snow attenuation theory and calculations at lower frequencies.

Gunn and East⁴² give an equation for snow attenuation for wavelengths greater than 1.5 cm where the Rayleigh approximation applies, i.e., the equivalent water sphere sizes derived by melting snowflakes are smaller than the wavelength; for 0° C the equation is

$$\alpha_s = 0.00349 \frac{R^{1.6}}{\lambda^4} + 0.00224 \frac{R}{\lambda} \quad (21)$$

⁴⁰Babkin, Yu. S., Iskhakov, I.A., Sokolov, A.V., Stroganov, L.I., and Sukhonin, Ye. V., "Attenuation of Radiation at a Wavelength of 0.96 MM in Snow," Radio Eng. and Elec. Phys., 15, 12, 2171-2174, 1970.

⁴¹Sokolov, A.V., "Attenuation of Visible and Infrared Radiation in Rain and Snow," Radio Eng. and Elec. Phys., 15, 12, 2175-2178, 1970.

⁴²Gunn, K.L.S., and East, T.W.R., "The Microwave Properties of Precipitation Particles," Quart. J. Roy. Meteor. Soc., 80, 533-545, Oct 1954.

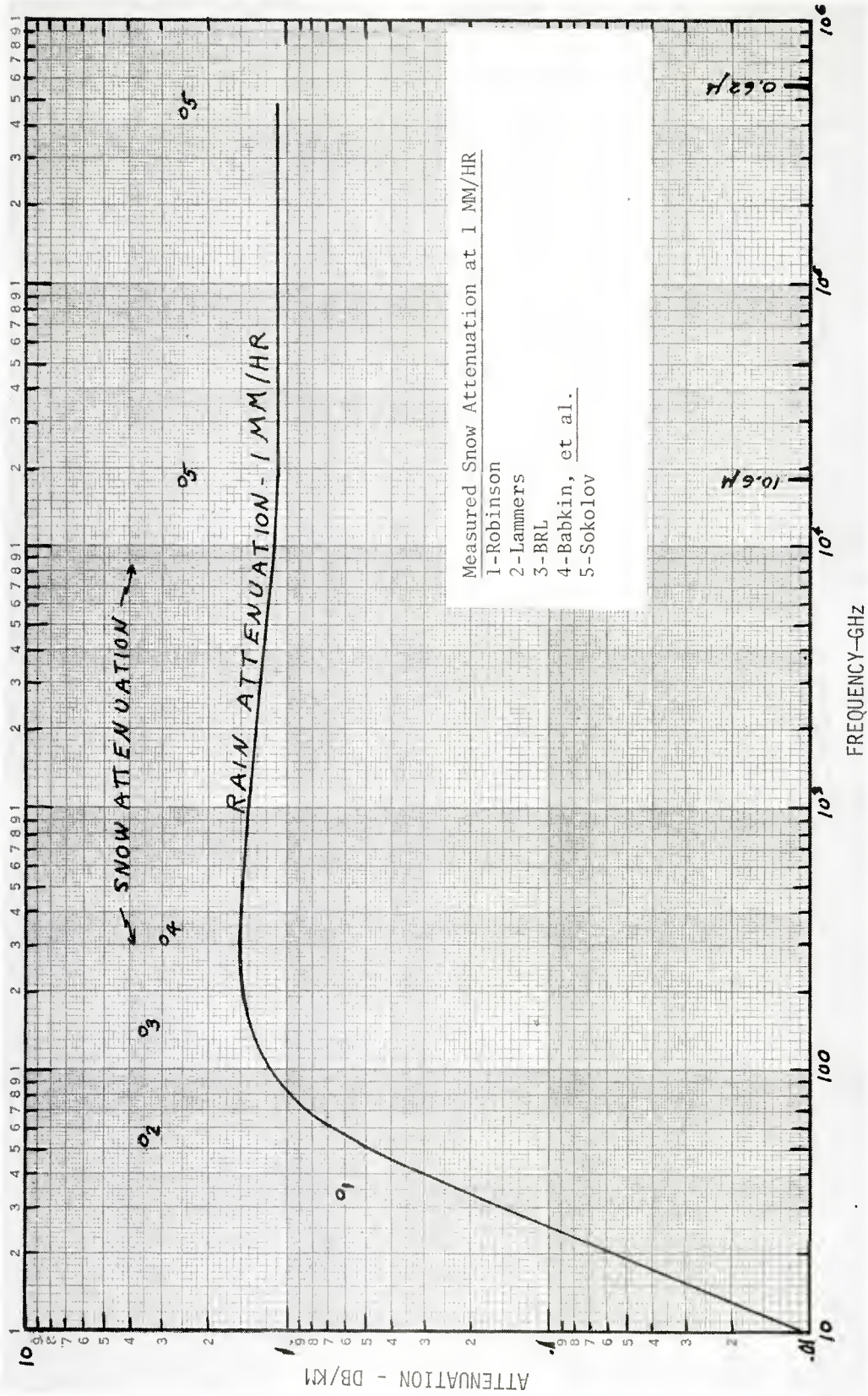


Figure 27. Measured Snow Attenuation Versus Frequency

where λ is the wavelength in cm. The applicable temperature is given as 0° C, but, in practice, for equation (21) to apply, the snow must be completely dry with no trace of melting since an index of refraction for a mixture of only ice and air was assumed.

There is a temperature dependence for snow attenuation below freezing because of the decrease in the absorption coefficient of ice with decreasing temperature. Cumming⁴³ has reported that the absorption coefficient of ice is nearly independent of wavelength in the centimetre band and Lammers^{38,39} extends this constancy to millimetre wavelengths. The absorption coefficient of ice, from Cumming,⁴³ is 24×10^{-4} at 0°, 7.9×10^{-4} at -10° and 5.5×10^{-4} at -20° C. Thus, there is a decrease by a factor of 4.4 in the absorption coefficient between 0° and -20° C.

Using equation (21), the attenuation of snow at 16 GHz and 1 mm/hr equivalent rainfall rate is 1.6×10^{-3} dB/km at 0°, 0.73×10^{-3} at -10°, and 0.51×10^{-4} at -20° C. These are very small attenuation values compared with 0.03 dB/km attenuation of rain at this frequency.

Lammers^{38,39} has reported in considerable detail on the theory of snow attenuation at millimetre wavelengths including some measured data at 35 GHz for wet snow. His calculations of snow attenuation are based on measured snowflake size distribution data by Gunn and Marshall,⁴⁴ from which equivalent water sphere sizes were derived. Complex index of refraction of snow for an ice-air mixture was used along with exact Mie theory derived total loss cross sections of snow and falling speeds of snowflakes by Langleben.⁴⁵ The attenuation of dry snow with a density of 0.05 g/cm^3 and an equivalent rainfall of 1 mm/hr is given as 0.01 dB/km; rain attenuation would be 0.5 dB/km.

Lammers states that measurements on snow, "which scarcely displays any moisture after falling," agree with his calculated values. Measurements on wet snow at 53 GHz are reported to be as high as 3.5 dB/km at 1 mm/hr which is 5.8 times higher than rain attenuation.

⁴³Cumming, W.A., "The Dielectric Properties of Ice and Snow at 3.2 Cm," *J. Appl. Phys.*, 23, p768, 1952.

⁴⁴Gunn, K.L.S. and Marshall, J.S., "The Distribution of Size of Aggregate Snowflakes," *J. Meteor.*, 15, p452, 1958.

⁴⁵Langleben, M.P., "The Terminal Velocity of Snow Aggregates," *Quart. J. Roy. Meteor. Soc.*, 80, p174, 1954.

Babkin et al⁴⁰ calculated and measured snow attenuation at 312.5 GHz with a density of 0.07 g/cm^3 over a range of equivalent rainfall rates up to 2 mm/hr. Their calculations were based on Gunn and Marshall's⁴⁴ snowflake size distribution function and complex index of refraction of an ice-air mixture using data on ice from Kislovski,⁴⁶ Steineman and Granicher,⁴⁷ and Smyth and Hitchcock.⁴⁸ The measured attenuation of snow with a density of 0.07 g/cm^3 was reported to be 5 to 6 times higher than calculated and is about twice rain attenuation. By arbitrarily doubling the size of the water drops formed by melting snowflakes, calculated attenuation would agree with measured attenuation, indicating that it is not entirely the water content of the snowflakes but also the shape that determines the attenuation.

Asari⁴⁹ has evaluated the dielectric constant of snow as it exists in various physical forms including ball, powder, wind-blown, cotton I, cotton II, button, and packed types. The scattering cross section and attenuation are computed for these various types of snow at 11, 15, 24 and 35 GHz.

IV. CONCLUSION

Experimental data on the 140-GHz attenuation and visibility of fog, rain, and snow have been obtained that are useful for evaluating the performance of millimetre wave systems under adverse weather conditions.

Empirically derived equations expressing the relationships between the attenuation of fog, rain, and snow and the rainfall rate or visibility have been developed. The agreement between the measured and theoretically derived data is generally good. The measured fog attenuation is somewhat higher than calculated for radiation type fog and tended to match advection fog conditions. This is not unreasonable since the propagation path was over low ground adjacent to marshland and not far from a large body of water.

The measured rain attenuation regression curve matches the calculated curve using the Laws and Parsons drop-size distribution between 5 and 20 mm/hr but is somewhat lower at lower rainfall rates.

⁴⁶Kislovskiy, L.K., *Optics and Spectroscopy*, No. 1, p672, 1956.

⁴⁷Steineman, A. and Granicher, H., *Helv. Phys. Acta.*, 30, p553, 1957.

⁴⁸Smyth, C.P., and Hitchcock, C.S., *J. Am. Chem. Soc.*, 54, p4631, 1932.

⁴⁹Asari, E., "Propagation in Snow," *Electronics and Communications in Japan*, 52-B, 11, 69-76, 1969.

Wet snow attenuation was much larger than rain attenuation for the same equivalent rainfall rate which could not be checked against any other data at 140 GHz, but other experiments at lower and higher frequencies gave similar results.

The data on visibility are useful for evaluating systems performance under limited visibility conditions, particularly when a choice of the use of optical or millimetre wavelengths must be made.

The attenuation caused by rain on the lucite window is indicative of the losses that can occur with a radome. Care must be taken to insure a non-wetting surface with rapid run-off of accumulated water.

Winds with a vertical component will change the raindrop density and, therefore, the attenuation of rain quite significantly, causing wide and possibly rapid variations in the attenuation if the wind is gusty. The presence of vertical winds contributes to the extremely wide scatter of measured attenuation sometimes observed.

Brief resumes of the scope and results of theoretical studies by other authors on millimetre wave propagation attenuation have been presented to serve as a basis of comparison with measured data and to provide supplementary data and explanations of observed phenomena.

A composite graph of the attenuation of fog, rain, snow and the normal, fair-weather atmosphere as a function of frequency is shown in Figure 28. The relative magnitude of the effects of the various factors that can cause attenuation in atmospheric propagation can be conveniently assessed in this graph.

The fog data in Figure 28 are from Reference 12. The rain data extrapolated from Setzer's³² calculations match most measured data quite well. The snow data are from Figure 27 and the atmospheric data are from Rozenblum.⁵⁰ The actual attenuation will be the sum of the attenuation values for each pertinent factor.

The atmospheric attenuation curve in Figure 28 is for a water vapor density of 7.5 g/m^3 at 20° C which corresponds to a relative humidity of 42%. The atmospheric attenuation at 140 GHz is almost entirely due to water vapor, oxygen attenuation is less than 0.1 dB/km. Water vapor attenuation is almost linearly proportional to the water vapor density and care must be taken to use the actual atmospheric conditions when evaluating attenuation. The relationship between 140-GHz water vapor attenuation, relative humidity, and temperature is shown in Figure 29.

⁵⁰Rozenblum, E.S., *Atmospheric Absorption of 10-400 KCPS Radiation; Summary and Bibliography to 1960*, "MIT, Lincoln Lab. Rpt. 826-0021, Aug 15, 1960, AD 242 598; also, Microwave Journal, Mar 1961.

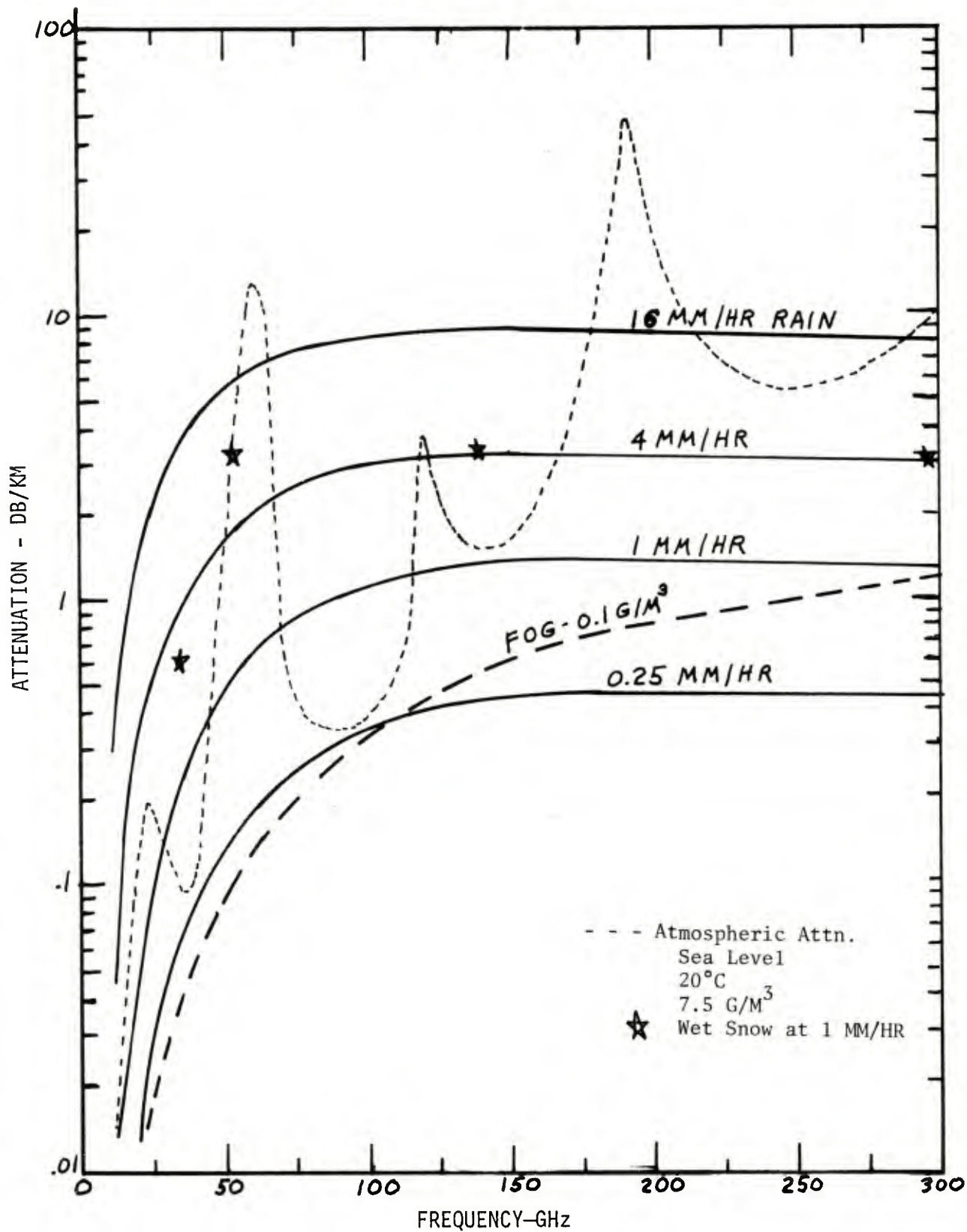


Figure 28. Rain, Fog, and Atmospheric Attenuation Versus Frequency

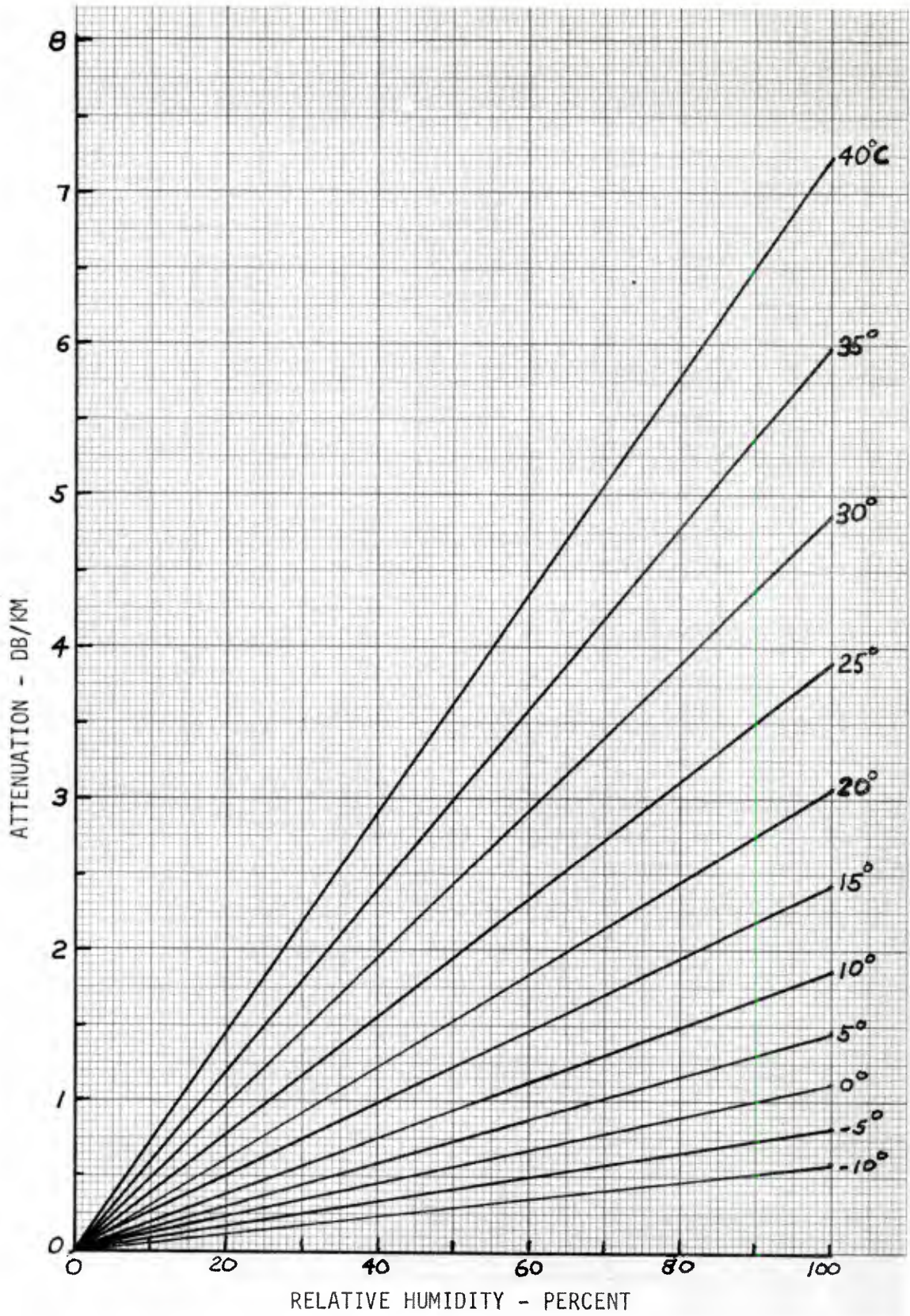


Figure 29. 140 GHz Water Vapor Attenuation Versus Relative Humidity and Temperature

A water vapor attenuation coefficient of 0.18 dB/km/g/m³ at 20°C was used which was derived from measurements at BRL. Tolbert, et al.⁵¹ reported on a measured attenuation coefficient of 0.25 dB/km/g/m³, which from experience at BRL seems to be too high.

Aganbekyan, et al.⁵² have reported that the attenuation coefficient of water vapor decreases with increasing temperature in the millimetre wavelength propagation window at 140 GHz as

$$\alpha_T = \alpha_{293} \left(\frac{T}{293}\right)^{-3.5} \quad (22)$$

where α_T \equiv attenuation coefficient in dB/km at absolute temperature T
 α_{293} \equiv attenuation coefficient in dB/km at 293° K.

The water vapor density as a function of relative humidity was determined from the equation

$$\rho_V = 2.17 \left(\frac{e_s}{T}\right) f \quad (23)$$

where ρ_V \equiv water vapor density, g/m³

e_s \equiv saturation water vapor density over water, millibars, at temperature T

f \equiv relative humidity, percent.

It should be noted that the water vapor attenuation is quite large at high temperatures and high relative humidity; it may exceed light and medium rain attenuation.

⁵¹ Tolbert, C.W., Straiton, A.W., and Douglas, J.H., "Studies of 2.15 MM Propagation at an Elevation of 4 KM and the Millimeter Absorption Spectrum, EERL Rpt. No. 103, Univ. of Texas, TX, 1 Nov 1958.

⁵² Aganbekyan, K.A., Zrazhevskiy, A. Yu., and Malinkin, V.G., "Temperature Dependence of the Absorption of Radio Waves by Atmospheric Water Vapor at the 10 cm - 0.27 mm Wavelengths, Radio Eng. and Elect. Phys., 20, 1-6, Nov 1975.

V. ACKNOWLEDGEMENTS

The experimental program described in this report is the result of the efforts of a number of persons in the group doing millimeter wave research at the Ballistic Research Laboratory. Particular credit is due Harvey LaFon who participated in the design, installation and operation of the experiment. The rain attenuation data obtained without the lucite windows were measured by Donald Bauerle, Joe Knox, and Bruce Wallace.

REFERENCES

1. Middleton, Visibility Through the Atmosphere, Univ. of Toronto Press, 1958.
2. Robinson, N.P., "Measurements of the Effect of Rain, Snow, and Fogs on 8.6 mm Radar Echoes," Proc. IEE, London, 102B, Paper No. 189R, 709-714, Sep 1955.
3. Lukes, G.D., "Penetrability of Haze, Fog, Clouds, and Precipitation on Radiant Energy Over the Spectral Range 0.1 Micron to 10 Centimeters," The Center for Naval Analyses, Univ. of Rochester, Study No. 61, May 1968. AD 847 658
4. Koester, K.L. and Kosowsky, L.H., "Attenuation of Millimeter Waves in Fog," 14th Radar Meteorology Conf., Tucson, AZ, 17-20 Nov 1970; also, Norden Div of United Aircraft Corp., Rpt X31051, 10 Aug 1970.
5. Koester, K.L. and Kosowsky, L.H., "Millimeter Wave Propagation in Fog," IEEE, Ant. and Prop. Symp., 20-24 Sep 1971, Los Angeles, CA; Norden Div United Aircraft Rpt X31059, 14 Jun 1971.
6. Ryde, J.W. and Ryde D., "Attenuation of Centimeter and Millimeter Waves by Rain, Fog, and Clouds," Tech Rpt 8670, British General Electric Co., Wambly, England, May 1945; also, earlier report, GEC No. 7831, Oct 1941, Ryde and Ryde. See also C.R. Burrows and S.S. Atwood, Radio Wave Propagation, Academic Press, NY, Vol II, Chap 5, 1949.
7. Kerr, D.E., Propagation of Short Radio Waves, McGraw-Hill, 11, NY, 1951.
8. Skolnik, M., Introduction to Radar Systems, McGraw-Hill, NY, 1962.
9. Eldridge, R.G., "Haze and Fog Aerosol Distributions," J. Atmospheric Sci., 23, 605-613, 1966.
10. Mason, E.J., The Physics of Clouds, Oxford, Clarendon Press, 1957.
11. Atlas, D. "Advances in Radar Meteorology," Advances in Geophysics, Vol 10, 317-478, Academic Press, NY, 1964.
12. Saxton, J.A. and Lane, J.A., "The Anomalous Dispersion of Water at Very High Radio-Frequencies," Meteorological Factors in Radiowave Propagation, Physical Society, London, Parts I, II and III, 1946.
13. Saxton, L.A., "Dielectric Dispersion in Pure Polar Liquids at Very High Radio-Frequencies, II. Relation of Experimental Results to Theory," Proc. Royal Soc., A, 213, p 473, 1952.

REFERENCES

14. Lane, J.A. and Saxton, J.A., "Dielectric Dispersion in Pure Polar Liquids at Very High Radio-Frequencies. I. Measurements of Water, Methyl, and Ethyl Alcohols," Proc. Royal Soc., 213, p 400, 1952; also, J. Opt. Soc. Proc. Royal Soc. Am., 56, No. 10, p 1398, 1966.
15. Chamberlain, J.E., et al, "Submillimetre Absorption and Dispersion of Liquid Water," Nature, 210, 790-791, May 21, 1966.
16. Deirmendjian, D., "Complete Microwave Scattering and Extinction Properties of Polydispersed Cloud and Rain Elements," The Rand Corp., R-422-PR, Dec 1963.
17. Deirmendjian, D., Electromagnetic Scattering and Spherical Polydispersions, American Elsevier Pub. Co. Inc., NY, 1969.
18. Mitchell, R.A. "Radar Meteorology of Millimeter Wavelengths," Aerospace Corp., Rpt TR-699(6236-46)-9, Air Force Rpt SSD-TR-66-117, Jun 1966. AD 488 085.
NOTE: Fig. 4, rain attenuation at 1 mm wavelength, is in error according to Mitchell's later report, "Remote Sensing of Rain by Radar," TR-0158(3525-09)-1, AF No. SAMSO-TR-68-115, Jan 1968.
19. Stanevich, A.E., and Yaroslavskii, N.G., "Absorption of Liquid Water in the Lone-Wavelength Part of the Infrared Spectrum (42-2000 microns)," Optics and Spectroscopy, 10, 278-279, Apr 1961.
20. Malyshenko, Y.I. and Wachser, I.K., "Calculation of the Dielectric Constant of Water in the Submillimetre Range of Radio Waves," Ukrain. Phys., 15, No. 5, 1970.
21. Chu, T.S., and Hogg, D.C. "Effects of Precipitation at 0.63, 3.5, and 10.6 Microns," BSTJ, 47, No. 5, 723-759, May-Jun 1968.
22. Dudzinsky, S.J., "Atmospheric Effects on Terrestrial Millimeter-Wave Communications," Rand Corp., Rpt R-1335-ARPA, Mar 1974.
23. Wilcox, F., "Millimeter Wave Radar," Proj. No. 1709-74-D6, JERA-2048, Goodyear Aerospace Corp., Arizona Division, Litchfield Park, AZ, 85340, 10 Apr 75.
24. Rogers, T.F., "An Estimate of the Influence of the Atmosphere on Airborne Reconnaissance Radar Performance," Prop. Lab., Air Force Cambridge Reas. Ctr., 4 Jan 1953.
25. Tolbert, C.W. and Gerhardt, J.R. and Bahn, W.W., "Rainfall Attenuation of 2.15 MM Radio Wavelength," EERL Rpt 109, Univ. of Texas, Austin, TX, 12 Jun 1959.

REFERENCES

26. Sander, J., "Research on the Attenuation of Electromagnetic Waves by Rain with 52, 90.8, and 150 GHz," Doctoral Engineering Dissertation, Tech. Univ., Berlin, D83. Translation, US Army Foreign Science and Technology Center, FSTC-HT-23-299,75, DIA Task No. T741801, 27 Mar 75.
27. Sander, J., "Rain Attenuation of Millimeter Waves at $\lambda = 5.77, 3.3,$ and 2 mm," IEEE Trans. Ant. & Prop., AP-23, 2, 213-220, Mar 75.
28. Zuffrey, C.H., "A Study of Rain Effects on Electromagnetic Waves in the 1-600 GHz Range," Master's Thesis, Dept Electrical Engineering, Univ. of Colorado, 1972.
29. Laws, O.J. and Parsons, D.A., "The Relation of Raindrop Size to Intensity," Trans. Am. Geophysical Union, Vol 24, 452-460, 1943.
30. Marshall, J.S. and Palmer, W. McK. "The Distribution of Raindrops With Size," Journ. of Meteorology, Vol. 5, 165-166, Aug 1948.
31. Lammers, U.H.W., "Electrostatic Analysis of Raindrop Distributions," J. Appl. Meteor., 8, 3, 330-334, 1969.
32. Setzer, D.E., "Computed Transmission Through Rain at Microwave and Visible Frequencies," BSTJ, 49, p1873-, 1970.
33. Sokolov, A.V. and Sukhonin, Ye. V., "Attenuation of Submillimetre Radio Waves in Rain," Radio Eng. and Elec. Phys, 15, 12, 2167-2171, Dec 1970.
34. Polakova, Ye. A., "Investigation of the Microstructure of Rains in Connection with the Question of Their Transparency," Trans. (Trudy GCO), Proc. of the Main Geophysical Observatory, Issue 220, Chap. 2, Sec 4, (Gidrometacizdat) 1967.
35. Rozenberg, V.I., "Radar Characteristics of Rain in Submillimetre Range," Radio Eng. and Elec. Phys., 15, 12, 2157-2163, Dec 1970.
36. Best, A.C., "The Size Distribution of Raindrops," Quart. J. Roy. Soc., 76, 16-36, 1950.
37. Naumov, A.D. and Stankevich, V.S., "On the Attenuation of Millimetre and Submillimetre Radio Waves in Rain," (Izv. Vuz), Radio Phys. & Quantum Elec., 145-147, Feb 1969.
38. Lammers, U. "Investigations on the Effects of Precipitation of MM-Wave Propagation," Doctoral-Engineering Dissertation, Tech. Univ., Berlin, D83, 1965. Translation by US Army Foreign Science and Technology Center, FSTC-HT-23-0298-75, DIA Task No. T741801, 1975.

REFERENCES

39. Lammers, U., "The Attenuation of MM-Waves by Meteorological Precipitation," Nachr. Tech. Z., 19, 1956 and NTZ-Commun. Jour., 16, No. 5-6, 1967.
40. Babkin, Yu. S., Ishakov, I.A., Sokolov, A.V., Stroganov, L.I., and Sukhonin, Ye. V., "Attenuation of Radiation at a Wavelength of 0.96 MM in Snow," Radio Eng. and Elec. Phys., 15, 12, 2171-2174, 1970.
41. Sokolov, A.V. "Attenuation of Visible and Infrared Radiation in Rain and Snow," Radio Eng. and Elec. Phys., 15, 12, 2175-2178, 1970.
42. Gunn, K.L.S., and East, T.W.R., "the Microwave Properties of Precipitation Particles," Quart. J. Roy. Meteor. Soc., 80, 533-545, Oct 1954.
43. Cumming, W.A., "The Dielectric Properties of Ice and Snow at 3.2 Cm," J. Appl. Phys., 23, p768, 1952.
44. Gunn, K.L.S. and Marshall, J.S., "The Distribution of Size of Aggregate Snowflakes," J. Meteor., 15, p452, 1958.
45. Langleben, M.P., "The Terminal Velocity of Snow Aggregates," Quart. J. Roy. Meteor. Soc., 80, p174, 1954.
46. Kislovskiy, L.D., Optics and Spectroscopy, No. 1, p672, 1956.
47. Steineman, A. and Granicher, H., Helv. Phys. Acta., 30, p553, 1957.
48. Smyth, C.P., and Hitchcock, C.S., J. Am. Chem. Soc., 54, p4631, 1932.
49. Asari, E., "Propagation in Snow," Electronics and Communications in Japan, 52-B, 11, 69-76, 1969.
50. Rozenblum, E.S., "Atmospheric Absorption of 10-400 KMCPS Radiation; Summary and Bibliography to 1960," MIT, Lincoln, Lab. Rpt. 826-0021, Aug 15, 1960, AD 242 598; also, Microwave Journal, Mar 1961.
51. Tolbert, C.W., Straiton, A.W. and Douglas, J.H., "Studies of 2.15 MM Propagation at an Elevation of 4 KM and the Millimeter Absorption Spectrum," EERL Rpt. No. 104, Univ. of Texas, Austin, TX, 1 Nov 1958.
52. Aganbekyan, K.A., Zrazhevskiy, A. Yu, and Malinkin, V., "Temperature Dependence of the Absorption of Radio Waves by Atmospheric Water Vapor at the 10 cm - 0.27 mm Wavelengths," Radio Eng. & Elect. Phys., 20, 1-6, Nov 1975.

BIBLIOGRAPHY

PROPAGATION AT AND ABOVE 140 GHZ

Survey and Literature Search Reports

1. DDC Report Bibliography, "MM Wave Propagation," DDC Search Control No. 023540, Nov 1974.
2. Hunt, W.T., "Survey of Attenuation by the Earth's Atmosphere at Millimeter Radio Wavelengths," Wright Air Dev. Div., USAF, Tech Note 60-232, Nov 1960. AD 252126.
3. Lurge, J., "Survey of the Literature on Millimeter and Submillimeter Waves," TRG-127-SR-2 for AFCRL, SR No. 2, June 30, 1960. AD 243342.
4. National Tech. Info. Service (NTIS), U. S. Dept. of Commerce, Springfield, VA 22151, "Millimeter Wave Rain Attenuation and Back-Scatter," March 11, 1975.
5. NASA Literature Search, "Attenuation and Backscattering of Millimeter Waves in the Atmosphere," NASA Science and Technical Information Division, P.O. Box 33, College Park, MD 20740, NASA Lit. Search No. 27541, 20 Nov 1974.
6. Straiton, A.W., Scarpero, D.C. & Vogel, W., "A Survey of Millimeter Wavelength Radio Propagation Through the Atmosphere," EERL, U. Texas, Austin, TR No. 68-1, 30 Nov 1968, AD 844946L.
7. Vogler, L. W. & Van Horn, S.F., "Bibliography on Propagation Effects from 10 to 1000 GHz," OT/TRER 30, OT, U.S. Dept. of Comm., March 1972.

Theoretical and Experimental Reports

8. Agabekyzn, K.A., Zrazhevskiy, A. Ju., Kolosov, M.A., Sokolov, A.V., "Study of the Absorption Dependence upon the Air Pressure at the Wave Length of 0.29, 0.36 and 0.45mm." Radio Eng. & Elect. Phys., 16, 8, P 1564, 1971.
9. Aganbekyna, K.A., Zrazhevskiy, A. Yu., Kolosov, M.A., and Sokolov, A.V., "Procedure and Results of Measurements of Absorption Coefficients of Submillimeter Radiation in Atmospheric Water Vapors," Proc. 9th All-Union Conference on Radiowave Propagation, Pt. II, p. 126, June, 1969.

BIBLIOGRAPHY (CONT.)

10. Babkin, Yu. S., Zimin, N.N., Izyumov, A.O., Sukhonin, Ye. V., & Shabalin, G. Ye., "Measurement of Attenuation in Rain Over 1 km Path at a Wavelength of 0.96mm," Radio Eng. & Elect. Phys., 15, 12, 2164-2166, Dec 1970.
11. Babkin, Yu.S., Izyumov, A.O. Smol'yaninova, L.I., Sokolov, A.V., Stroganov, L.I., & Sukhonin, Ye.V., "Investigation of Absorption of Submillimeter Waves in 850-960 μm range in the Atmosphere," Proc. 8-th All-Union Conference on Radiowave Propagation, 1967.
12. Basharinov, A. E. and Kutuza, B. G., "Study of the Radio Emission and Absorption of Waves of the Millimeter and Center Bands in a Cloudy Atmosphere," Trans. (Trudy) Main Geophys. Obs., No. 222, 1968.
13. Breeden, K. H., Rivers, W. K., and Sheppard, A. P., "Atmospheric Attenuation at Submillimetre Wavelengths," Electronics Letters, 2, 3, p. 88, Mar 1966.
14. Burroughs, W. J., Pyatt, E. C., and Gebbie, H. A., "Transmission of Sub-millimetre Waves in Fog," Nature, 212, No. 5060, 387-388, Oct. 22, 1966.
15. Chang, S. Y. and Lester, J. D., "Atmospheric Attenuation Measurements at 600 GHz," Memo Rpt M67-4-1, Frankford Arsenal, Philadelphia, PA August 1966. Also in IEEE, April 1966.
16. Chang, S. Y. and Lester, J. D., "Performance Characteristics of a 300 GHz Radiometer and Some Atmospheric Attenuation Measurements," IEE Trans. Ant. & Prop., AP-16(5), 588-591, 1968.
17. Coates, G. T., Bond, R. A., and Tolbert, C. W., "Propagation Measurements in the Vicinity of the 183 Gc/s Water Vapor Line," EERL, Univ. of Texas, Austin, Rpt No. 7-20, February 5, 1962.
18. Crane, R. K., "Propagation Phenomena Affecting Satellite Communications Systems Operating in the Centimeter and Millimeter Wavelength Bands," Proc. IEEE, 59, 2, 173-188, Feb 1971.
19. Crawford, A. B., and Hogg, D. C., "Measurement of Atmospheric Attenuation at Millimeter Wavelengths," Bell Sys. Tech. J., 35, 907-915, July 1956.
20. Emery, R., "Atmospheric Absorption Measurements in the Region of Imm Wavelength," Infrared Physics, 12, 65-79, 1972.

BIBLIOGRAPHY (CONT.)

21. Evans, A., Bachynski, M. P., and Wachter, A. G., "The Radio Spectrum from 10Gc to 300Gc in Aerospace Communications; Vol. IV - Absorption in Planetary Atmospheres and Sources of Noise," Tech. Rpt ASD-TR-61-589, Vol IV, RCA Victor Co., Ltd., Research Labs, Montreal, Canada, Aug. 1962. AD 294 452.
22. Gibbons, C. J., Gordon-Smith, A. C. & Gebbie, H.A., "Anomalous Absorption in the Atmosphere for 2.7mm Radiation," Nature, Vol. 243, 397-398, 15 June 1973.
23. Gurvich, A. S. and Naumov, A. P., "Theoretical Possibilities for Determining the Moisture Content of the Atmosphere through the Thermal Radio Emission in the Submillimeter Range," Atmos. and Oceanic Phys., 8, 307-309, May 1972.
24. Hoffman, L. A., "Millimeter-Wave Propagation and Systems Considerations," Aerospace Corp. Rpt. No. TR-0200 (4230-46)-1, SAMSO-TR-68-445, Oct 1968.
25. Hoffman, L. A., Hartwick, T. S., & H. J. Wintroub, "A Comparison of Millimeter and Laser Space-to-Space Communication Links," Aerospace Corp., SAMSO-TR-70-329, 31 Aug 1970.
26. Kammerer, J. E. & Richer, K. A., "140GHz Millimetric Bistatic Continuous Wave Measurements Radar," Ballistic Research Lab., APG, MD. Memo Rpt 1730, Jan 1966. AD484 693.
27. Kolosov, M. A., Sokolov, A. V. & Vvedenshii, B. A., "Investigations of the Propagation of Meter, Decimeter, Centimeter and Submillimeter Radio Waves," Radio Eng. & Elect. Phys., 12, 11, 1752-1771, Nov 1967.
28. Kolosov, M. A., & Sokolov, A. V., "Certain Problems of Propagation of Millimeter and Submillimeter Radiowaves," Radio Eng. and Elect. Phys., 15, 4, 563-570, Apr 1970.
29. Krasnyuk, N. P., Rozenberg, V. I. & Chistyakov, D. A., "Effect of Different Distributions of Raindrop Sizes on Radar Performance," 13, 5, 679-681, Radio Eng. & Elect. Phys., May 1968.
30. Krasnyuk, N. P. Rozenberg, V. I. & Chistyakov, D. A., "Attenuation and Scattering of Radio Waves by Raindrops of Various Origins," Atmos. & Ocean. Phys., 4, 11, 693-695, Nov. 1968.

BIBLIOGRAPHY (CONT.)

31. Krasnyuk, N. P. Rozenberg, V.I., & Chistyakov, D. A., "Attenuation and Scattering of Radar Signals by Rains With Shifrin and Marshall-Palmer Drop Size Distributions," Radio Eng. & Elect. Phys., 13, 10, 1638-1440, Oct. 1968.
32. Krasnyuk, N. P., Rozenberg, V. I., Chistyakov, D. A., "Attenuation and Dissipation of Electromagnetic Waves by Rain of Different Nature," Radio Phys. & Quant. Elec., 12, 10, 54-59, Oct. 1969. AD847658.
33. Krasnyuk, N. P. Rozenberg, V.I., & Chistyakov, D. A., "Radar Characteristics of Precipitation of Different Nature, Spectra, Intensity and Temperatures in the Centimeter and Millimeter Ranges of Radio Waves," FTD-MT-24-246-69, Trans. Div. Foreign Tech. Div., WPAFB, 29 Oct 1969. AD 700401
34. Kukin, L. M., Lubyako, L.V., and Fedoseyev, L. I., "Measurement of Atmospheric Absorption in 1.8-0.87mm Range," Radio Phys. & Quant. Elect., 10, 6, 747, 1967.
35. Lane, J. A., Gordon-Smith, and Zavody, A. M., "Absorption and Scintillation Effects of 3mm Wavelength on a Short Line-of-Sight Radio Line," Electronic Letters, 3, 185-186, 1967.
36. Liebe, H. J. & Welch, W. M., "Molecular Attenuation and Phase Dispersion Between 40 and 140 GHz for Path Models from Different Altitudes," U. S. Dept of Commerce, Office of Telecommunications, OT Rpt. 73-10, May 1973.
37. Llewellyn-Jones, D. T., and Zavody, A.M., "Rainfall Attenuation at 110 and 890 GHz," Electronic Letters, 7, 12, June 17, 1971.
38. Malishko, Yu. I., "Absorption Factor Measurement of Water Vapour in the 1.3mm Transparency Window," Radio Eng. & Elect. Phys., 14, 3, 522-523, Mar 1969.
39. Malishenko, Yu. I., Vakser, I. Kh., "Measurement of the Attenuation Coefficient at 1.3 and 0.86mm in Showers," Radio Phys. & Quant. Elect., 14, 6, p.258, June 1971.
40. Mitchell, R. L., "Remote Sensing of Rain by Radar," Aerospace Corp., Report No. TR-0158 (3525-09)-1, Air Force Rpt No. SAMSO-TR-68-115, Jan 1968.
41. Mitchell, R. L., "Scattering and Absorption Cross Sections of Water Spheres at Millimeter Wavelengths," Aerospace Corp., El Segundo, CA Rpt TR-669 (6230-46)-11, 1966.

BIBLIOGRAPHY (CONT.)

42. Mondre, E., "Atmospheric Effects on Millimeter Wave Communication Channels," NASA, GSFC, X-733-70-250, Access. No. N70-34446, TMX-63985, Mar 1970.
43. Morgan, L. A., and Ekdahl, C. A., Jr., "Millimeter Wave Propagation," Tech. Rept. No. RADC-TR-66-342, Rome Air Development Center, Griffiss AFB, NY, 1966. AD 489 424.
44. Naumov, A. P. & Stankevich, V. S., "Attenuation of Millimeter and Submillimeter Radio Waves in Rains," Radio Phys. & Quant. Elect., 12, 2, 145-147, Feb 1969. NASA Rpt No. NASA-TT-F-12575, N69-36987.
45. Rogers, T. F., "An Estimate of Influence of the Atmosphere on Airborne Reconnaissance Radar Performance," Prop. Lab., AFCRC, 4 Jan 1953.
46. Rozenberg, V. I., "On Dielectric Penetrability of Water at 1.2 to 1.6 Millimeter Wavelength," Optics and Spectroscopy, 11, 2, 322-323, 1968.
47. Ryadov, V. Ya, Furashov, N. I., and Sharonov, G.W., "Measurement of Atmospheric Transparency to 0.87mm Waves," Radio Eng and Elect. Phys., 9, June 1964.
48. Ryadov, V. Ya. & Furashov, N. I., "Measurements of Atmospheric Absorption of Radiowaves in 0.76-1.15mm Range," Radio Phys. & Quant. Elect., 9, 5, p. 859, 1966.
49. Ryadov, V. Ya. & Sharonov, G. A., "Experimental Investigation of the Transparency of Earth's Atmosphere at Submillimeter Wavelengths," Radio Eng. & Elect. Phys., 11, p. 902, 1966.
50. Sander, J., "Computation of Attenuation of Electromagnetic Waves with $\lambda = 5.77, 3.3$ & 2mm With Special Attenuation to Raindrop Size Distribution," Tech. Rpt. 121, Heinrich Hertz Inst., Berlin-Charlottenberg, 1970.
51. Sander, J., "Investigations on the Attenuation of Electromagnetic Waves by Rain at 52, 90.8 and 150 GHz," (Untersuchungen zur Daempfung Elektromagnetischer Wellen durch Regen bei 52, 190.8 and 150 GHz) Tech Rept 153, Heinrich Hertz Inst., Berlin-W, 17 April 1972, NASA N74-11978/5.
52. Sander, J., "Rain Attenuation of Millimeter Waves at $\lambda=5.77, 3.3$ and 2mm," Heinrich-Hertz-Institut, Berlin-Charlottenburg, Germany, 1 Berlin 10, Einsteinufer 37. Final draft completed while a post-doctoral Fellow at RLE, MIT, 1973.

BIBLIOGRAPHY (CONT.)

53. Sander, J., "The Influence of Raindrop Size Distribution on the Attenuation of $\lambda=5.77, 3.3$ & 2mm Waves," Trans. by US Army Foreign Serv. Sci. & Tech. Ctr., FSTC-HT-23-0300-75, DIA Task No. T741801, 20 Feb 1975.
54. Sander, J., "Rain Attenuation of Millimeter Waves at $\lambda=5.77, 3.3$ & 2mm," IEEE Trans. Ant. & Prop., AP-23, 2, 213-220, March 1975.
55. Scarpero, C.C., "Atmospheric Effects on the Electromagnetic Wave Propagation in the Frequency Range 15-200 GHz," Masters Thesis, Univ. Texas, Austin, 1969.
56. Sokolov, A. V. and Skuhonin, Ye. V., "Problem of Attenuation of Radiowaves in 0.1-2mm Range by Rains of Different Intensity," Proc. 9th All-Union Conference on Radiowave Propagation, (Soviet), June, 1969.
57. Sokolov, A. V. & Sukhonin, Y. V., "Attenuation of Submillimeter Radio Waves in Rain," Radio Eng. & Elect. Phys., 15, 2167-2171, Dec 1970.
58. Sokolov, A. V. & Sukhonin, E. V., "Influence of the Atmosphere on the Propagation of Submillimeter Radio Waves," Submillimeter Waves; Proceedings of Symposium, New York, NY, Mar 31 - Apr 2, 1970, Polytechnic Press; NY.
59. Stanevich, A. E., & Yaroslavskii, N. G., "Absorption of Liquid Water in the Long-Wavelength Part of the Infrared Spectrum (42-2000 μ)" Optics and Spectroscopy, 10, 4, 278-279, April 1961.
60. Sheppard, A. P., "Atmospheric Attenuation in the Millimeter and Submillimeter Wavelength Region," Proc. Ninth Annual East Coast Conference on Aerospace and Navigational Electronics, pp. 6.2.2-1, Oct 1962.
61. Straiton, A. W. & Tolbert, C. W., "Anomalies in the Absorption of Radio Waves by Atmospheric Gases," Proc IRE, 48, 898-903, May 1960.
62. Straiton, A. W., & Ulaby, F. T., "Atmospheric Absorption of Radio Waves Between 150 and 350 GHz," IEEE Trans. on Ant. & Prop., Vol. AP-18, 479-485, July 1970.
63. Tillotson, L. C., "Millimeter Wavelength Radio Systems," Science, Vol. 170, No. 3, 31-36, Oct 2, 1970.
64. Tolbert, C. W., Straiton, A. W. & Douglas, J.H., "Studies of 2.15mm Propagation at an Elevation of 4km and the Millimeter Absorption Spectrum," TR No. 104, EERL, U. Texas, Austin, 1 Nov 1958.

BIBLIOGRAPHY (CONT.)

65. Tolbert, C.W., Britt, C.O. & Straiton, A.W., "2.15mm Radio Frequency Propagation Studies Over a 1.5 Km Path," TR No. 101, EERL, Univ. Texas, Austin, 15 July 1958.
66. Tolbert, C. W. & Straiton, A.W., "An Analysis of Recent Measurements of the Atmospheric Absorption of Millimetric Radio Waves," Proc. IRE, 49, No. 3, 649-500, Mar 1961.
67. Tolbert, C.W., Krause, L.C., & Bhan, W.W., "Solar Emission and Atmospheric Attenuation of 2.15 Millimeter Wave Length Radiation," EERL TR No. 5-41, Univ. Texas, Austin, 1960.
68. Tolbert, C.W., Straiton, A.W., Gerhardt, J.T., "A Study and Analysis of Anomolous Atmospheric Water Vapor Absorption of Millimeter Wavelength Radiation," TR No. 117, EERL, Univ Texas, Austin, Oct 1960.
69. Tolbert, C.W., Straiton, A.W. & Simons, R.W., "Attenuation and Emission of the Earth's Atmosphere Between the Frequencies of 100 and 160 Gc," EERL, Rpt. No. 5-55, Univ. Texas, Austin, 1964. AD 454390.
70. Tolbert, C.W., Krause, L.C. & Leeth, T. R., "Attenuation of the Earths Atmosphere Between the Frequencies of 100 and 140 GS/s," EERL, Univ. Texas, Austin, Rpt. No. 6, Oct 1963. AD-422 421.
71. Tolbert, C.W., Krause, L.C. & Straiton, A.W., "Attenuation of the Earth's Atmosphere Between the Frequencies of 100 and 140 Gigacycles per Second," J. Geophys. Res., 69(7), 1349-1357, 1964.
72. Tolbert, C.W. & Straiton, A.W., "Transmission Characteristics of Millimeter Radio Waves Between 100 and 260 GHz," Univ Texas, Austin, EERL, TR-68-47, Feb 1968, AD 828-953L.
73. Ulaby, F.T. & Straiton, A. W., "Atmospheric Attenuation Studies in the 183-325 GHz Region," IEEE Trans. Ant. & Prop., AP-17, (3), 337-342, 1969.
74. Ulaby, F.T. & Straiton, A.W., "Atmospheric Absorption of Radio Waves Between 150 and 350 GHz," IEEE Trans., AP-18, No. 4, 479-85. July 1970.
75. Usikov, O.K., German, V.L., & Vakser, I.K., "Investigation of the Absorption and Scatter of Millimeter Waves in Precipitation," Ukranian Phys. J., 6, 5, 618-641, 1961. Trans. FSTC-HT-23-284-75. NASA Rpt. NASA-TT-F-11913, N68-35837.

BIBLIOGRAPHY (CONT.)

76. Vakser, I.Kn., Malyshenko, Yu. I. & Kopilovich, L.E., "The Effect of Rain on the Millimeter and Submillimeter Radio Distribution," Atmos. & Oceanic Phys., 6, 9, 568-570, Sep 1970.
77. Vogel, W., "Scattering Intensity Plots and Transmission Coefficients for Millimeter Wave Propagation Through Rain," Univ. of Texas, Austin, TR-71-345, Dec 1971. AD 890-408L.
78. Vvedenskii, B.A., Kolosov, M.A., & Sokolov, A.V., "Investigations of the Propagation of Meter Decimeter and Submillimeter Radio Waves," Radio Eng. & Elect. Phys., 12, 11, 1752-1771, Nov 1967.
79. Whaley, T.W., "The Experimental Evaluation and Analysis of Free Space Propagation of Coherent Signals Between the Frequencies of 160 and 260 GHz," EERL, Univ of Texas, Austin, TR-3, Feb 1967, AD-808 516L.
80. Yaroslavsky, N.G. & Stanevich, A.E., "The Long Wavelength Infrared Spectrum of H₂O Vapor and the Absorption Spectrum of Atmospheric Air in the Region 20-2500 μ (500-4cm⁻¹)," Optics and Spectroscopy, 7, 380-382, 1959.
81. Zhevakin, S.A. & Naumov, A.P., "Absorption of Electromagnetic Radiation by Water Vapor on 10 μ -2cm Waves in the Upper Layers of the Atmosphere," Geomagnetism and Aeronomy, Vol 3, 537-546, 1963.
82. Zhevakin, S.A. & Naumov, A.P., "Coefficient of Absorption of Electromagnetic Waves by Water Vapor in Range 10 μ to 2cm," Radio Phys. & Quant. Elect., 6, 4, p. 674, Apr 1963.
83. Zhevakin, S.A. & Naumov, A.P., "Absorption of Centimeter and Millimeter Radio Waves by Atmospheric Water Vapor," Radio Eng. & Elect. Phys., 9, 8, 1097-1104, Aug 1964.
84. Zhevakin, S.A. & Naumov, A.P., "Calculation of Atmospheric-Oxygen Absorption Coefficients for Centimeter and Millimeter Radio Waves," Radio Eng. & Elect. Phys., 10, 6, June 1965.
85. Zhevakin, S.A. & Naumov, A.P., "The Propagation of Centimeter, Millimeter, and Submillimeter Radio Waves in the Earth's Atmosphere," Radiophysics & Quant. Elect., 10, 9 & 10, 678-694, Sep - Oct 1967, AD694 411.
86. Zoloterev, V.M., Mikhailov, B.A., Alperovich, L.I & Popov, S.I., "Dispersion and Absorption of Liquid Water in the Infrared and Radio Regions of the Spectrum," Optics and Spectroscopy, 27, 430-432, 1969.

DISTRIBUTION LIST

<u>No. of Copies</u>	<u>Organization</u>	<u>No. of Copies</u>	<u>Organization</u>
12	Commander Defense Documentation Center ATTN: DDC-TCA Cameron Station Alexandria, VA 22314	1	Director US Army Air Mobility Research and Development Laboratory Ames Research Center Moffett Field, CA 94035
2	Director of Defense Research and Engineering Engineering Technology ATTN: Mr. L. Weisberg Dr. D. Charvonia Washington, DC 20301	6	Commnader US Army Electronics Command ATTN: DRSEL-RD DRSEL-CT DRSEL-CT-R, Mr. Pearce DRSEL-NL-CR, M. J. Minx DRSEL-TL-ES, Mr. F. Rothwarf Fort Monmouth, NJ 07703
1	Director Defense Advanced Research Projects Agency ATTN: Dr. J. Tegnalia 1400 Wilson Boulevard Arlington, VA 22209	1	Office of the Test Director Joint Services LGW/CM Test Program ATTN: DRSEL-WL-MT, R. Murray White Sands Missile Range NM 88002
1	Director Institute for Defense Analyses 400 Army Navy Drive Arlington, VA 22202	1	Commander US Army Electronics Command Atmospheric Science Research ATTN: DRSEL-BL-RD Fort Huachuca, AZ 85613
1	Director Defense Nuclear Agency ATTN: STRA (RAEL), LTC Brown Washington, DC 20305	1	Director US Army Night Vision Laboratory Visionics Technical Area ATTN: DRSEL-NV-VI, J.R. Moulton Fort Belvoir, VA 22060
1	Commander US Army Material Development and Readiness Command ATTN: DRCDMA-ST 5001 Eisenhower Avenue Alexandria, VA 22333	4	Commander US Army Missile Research and Development Command ATTN: DRDMI-R, Mr. Pittman DRDMI-RBL DRDMI-RES DRDMI-RER, Mr. H. Green Redstone Arsenal, AL 35809
1	Commander US Army Aviation R&D Command ATTN: DRSAV-E 12th and Spruce Streets St. Louis, MO 63166		

DISTRIBUTION LIST

<u>No. of Copies</u>	<u>Organization</u>	<u>No. of Copies</u>	<u>Organization</u>
4	Commander US Army Missile Research and Development Command ATTN: DRDMI-RF, Mr. C. Hussey DRDMI-RFC, A. Michetti DRDMI-RFE, Mr. Salonimer DRDMI-RR, Mr. S. Johnston Redstone Arsenal, AL 35809	4	Commander US Army Armament Research and Development Command ATTN: DRDAR-SCF (2 cys) Mr. R. Phielsticker Mr. J. Schmitz Mr. S. Greenberg Dover, NJ 07801
1	Commander US Army Missile Research and Development Command Redstone Scientific Info Center ATTN: Chief, Document Station Redstone Arsenal, AL 35809	1	Director Rodman Laboratory ATTN: DRDAR-GSR Rock Island, IL 61202
1	Commander US Army Tank Automotive Development Command ATTN: DRDTA-RWL Warren, MI 48090	1	Commander US Army White Sands Missile Range ATTN: STEWS-TE, J. Flores White Sands, NM 88002
1	Commander US Army Mobility Equipment Research & Development Command ATTN: SMEFB-EM, K. Steinback Fort Belvoir, VA 22060	2	Commander US Army Harry Diamond Labs ATTN: DRXDO-TI DRXDO-RA, J. Salerno 2800 Powder Mill Road Adelphi, MD 20783
1	Commander US Army Armament Materiel Readiness Command ATTN: DRSAR-LEP-L, Tech Lib Rock Island, IL 61202	1	Commander US Army Foreign Science and Technology Center Federal Office Building 220 7th Street Charlottesville, VA 22901
2	Commander US Army Armament Research and Development Command ATTN: DRDAR-SE, J. Brinkman DRDAR-LCV-DE, Mr. Malgeri Dover, NJ 07801	1	Commander US Army Training and Document Command Fort Monroe, VA 23351

DISTRIBUTION LIST

<u>No. of Copies</u>	<u>Organization</u>	<u>No. of Copies</u>	<u>Organization</u>
1	Director US Army TRADOC Systems Analysis Activity ATTN: ATAA-SL, Tech Lib White Sands Missile Range NM 88002	1	Commander US Naval Air Systems Command ATTN: AIR-2324, Mr. C. Francis Washington, DC 20360
1	Commander US Army Combined Arms Development Activity Fort Leavenworth, KS 66027	1	Chief of Naval Research Department of the Navy Washington, DC 20360
1	Office of Assistant Secretary of the Army for R&D Assistant for Electronics ATTN: Mr. V. L. Friedrich Washington, DC 20310	1	Commander Center for Naval Analyses ATTN: Document Control 1401 Wilson Boulevard Arlington, VA 22209
1	HQDA (DAMA-CSM-CA) Washington, DC 20310	2	Commander US Naval Air Development Center ATTN: AETD, Radar Division Mr. M. Foral Warminster, PA 18974
1	HQDA (DAMA-DDZ-C) Washington, DC 20310	2	Commander US Naval Electronics Lab Ctr ATTN: Code 2330, J. Provencher Tech Library San Diego, CA 92152
1	Commander US Army Research Office ATTN: Dr. D. Van Hulsteyn P. O. Box 12211 Research Triangle Park, NC 27709	2	Commander US Naval Surface Weapons Center ATTN: Library Code DF34 Dahlgren, VA 22448
1	Commander TCATA ATTN: Scientific Advisor Fort Hood, TX 76544	3	Commander US Naval Weapons Center ATTN: Mr. R. Moore Mr. R. Higuera Dr. J. Battles, Code 6014 China Lake, CA 93555
1	Commander US Army Research and Development Group (Europe) ATTN: Electronics Branch Box 15 FPO New York 09510		

DISTRIBUTION LIST

<u>No. of Copies</u>	<u>Organization</u>	<u>No. of Copies</u>	<u>Organization</u>
2	Director US Naval Research Laboratory ATTN: Code 5370, Radar Geophysics Branch Code 5460, Electro- magnetic Prop Branch Washington, DC 20375	2	Director NASA Goddard Space Flight Center ATTN: Library Code 951, Mr. L. J. Ippolito Greenbelt, MD 20771
1	AFATL/DLB Eglin AFB, FL 32542	1	Director National Aeronautics and Space Administration Scientific and Technology Information Facility ATTN: Acquisitions Branch (S-AK/OL) P. O. Box 8757 Baltimore/Washington International Airport, MD 21240
1	AFATL/DLTG, F.H. Prestwood Eglin AFB, FL 32542		
1	AFATL/DLMT Eglin AFB, FL 32542		
2	AFATL (DLY/DLDG) Eglin AFB, FL 32542		
1	ADTC/ADBPS-12 Eglin AFB, FL 32542	2	Aerospace Corporation Electronics Research Laboratory ATTN: Mr. H. Kins Dr. R. L. Mitchell E1 Segundo, CA 90245
1	ADTC/ADA Eglin AFB, FL 32542		
1	RADC/EMATE Griffiss AFB, NY 13440	1	Bell Telephone Laboratories Crawford Hill Laboratory ATTN: Dr. D. C. Hogg Holmdel, NJ 07733
2	AFGL (LZ, Mr. C. Sletten; LZN, E. E. Altschuler) Hanscom AFB, MA 01731		
1	AFWL/DEV Kirtland AFB, NZ 87117	1	The Bendix Corporation Bendix Communications Division ATTN: Palmer H. Arnold East Joppa Road Baltimore, MD 21204
1	AFAL/WRW, Mr. Leasure Wright-Patterson AFB, OH 45433		
1	AFAL (RWN-1, Mr. Ray Bruns) Wright-Patterson AFB, OH 45433	1	Delphi Corporation ATTN: Mr. Lee Strom 1830 Massachusetts Avenue McLean, VA 22101
1	AFWL/TEM-4, CPT J. Schell Wright-Patterson AFB, OH 45433		

DISTRIBUTION LIST

<u>No. of Copies</u>	<u>Organization</u>	<u>No. of Copies</u>	<u>Organization</u>
1	Goodyear Aerospace Corporation Arizona Division ATTN: Mr. Fred Wilcox Litchfield Park, AZ 85340	1	The Rand Corporation ATTN: Dr. S. Dudzinsky, Jr. 1700 Main Street Santa Monica, CA 90406
1	Honeywell, Inc. Systems and Research Division ATTN: Mr. C. Seashore 2700 Ridgway Parkway Minneapolis, MN 55413	1	Raytheon Company Missiles Systems Division ATTN: Mr. Walter Justice Hartwell Road Bedford, MA 01730
1	Hughes Aircraft Company Aerospace Group Advanced Program Development Systems Division ATTN: P. B. Reggie Canoga Park, CA 91304	1	Sperry Rand Corporation Microwave Electronics Division ATTN: Mr. R. Roder Clearwater, FL 33518
1	Hughes Aircraft Company Aerospace Group Radar Division ATTN: Dr. R. Wagner Culver City, CA 90230	1	United Aircraft Division Norden Division ATTN: Dr. L. Kosowsky Helen Street Norwalk, CT 06852
2	Hughes Aircraft Company Aerospace Group Electron Dynamic Division ATTN: Mr. N. B. Kramer Mr. J. F. Sparacio 3100 W. Lomita Boulevard Torrance, CA 90504	4	Director Applied Physics Laboratory The John Hopkins University ATTN: Dr. A. Stone Dr. I. Katz Mr. J. Schneider Dr. C. Kilgus Johns Hopkins Road Laurel, MD 20810
1	LTV Aerospace Corporation Michigan Division ATTN: Dr. J. Mayersak P. O. Box 909 Warren, MI 48090	3	Georgia Institute of Tech Engineering Experiment Station ATTN: Dr. R. Hayes Dr. Fred Dyer Dr. N. Currie 347 Ferst Drive Atlanta, GA 30332
1	Martin Marietta Corporation ATTN: Dr. Jim Wiltse P. O. Box 5837 Orlando, FL 32805		

DISTRIBUTION LIST

<u>No. of Copies</u>	<u>Organization</u>	<u>No. of Copies</u>	<u>Organization</u>
1	Director MIT Lincoln Laboratory ATTN: Dr. R. K. Crane P.O. Box 73 Lexington, MA 02173	2	University of Texas at Austin Electrical Engineering Research Laboratory ATTN: Dr. A. Straiton Dr. R. Fannin Rt. 4, Box 198 Austin, TX 78751
1	South Dakota School of Mines and Technology Institute of Atmospheric Physics ATTN: Dr. Paul Smith Rapid City, SD 57701	1	University of Washington College of Engineering Department of Electrical Engineering ATTN: Dr. James C. Lin Seattle, WA 98145
1	Stanford Research Institute Electronics and Radio Sciences Division ATTN: Dr. R. Leadabrand 333 Ravens Wood Avenue Palo Alto, CA 94025		<u>Aberdeen Proving Ground</u> Marine Corps Ln Ofc Dir, USAMSAA Dir, USAMTD ATTN: STEAP-MT-TF Mr. W. Frazier
1	Syracuse University Department of Electrical Engineering ATTN: Dr. R. McFee Syracuse, NY 13210		Cdr, USATECOM ATTN: John Phillips
1	University of Arizona Institute of Atmospheric Physics ATTN: Dr. L. J. Battan Tucson, AZ 85721		
1	University of Miami Department of Meteorology ATTN: Dr. R. Lhermitte Coral Gables, FL 33134		